BIOTINYLATED PEPTIDE NANOFIBERS FOR MODULATING THE IMMUNE RESPONSE

A THESIS SUBMITTED TO
THE GRADUATE SCHOOL OF ENGINEERING AND SCIENCE
OF BILKENT UNIVERSITY
IN PARTIAL FULFILLMENT OF THE REQUIREMENTS FOR
THE DEGREE OF
MASTER OF SCIENCE
IN
MATERIALS SCIENCE AND NANOTECHNOLOGY

By

Şehmus Tohumeken

June 2016

BIOTINYLATED PEPTIDE NANOFIBERS FOR MODULATING THE IMMUNE RESPONSE

By Şehmus Tohumeken

June 2016

We certify that we have read this thesis and that in our opinion it is fully adequate, in scope and in quality, as a dissertation for the degree of Master of Science.

Ayşe Begüm Tekinay (Advisor)

Mustafa Ö. Güler

Melih Ö. Babaoğlu

Approved for the Graduate School of Engineering and Science

Levent Onural

Director of the Graduate School

ABSTRACT

BIOTINYLATED PEPTIDE NANOFIBERS FOR MODULATING THE IMMUNE RESPONSE

Şehmus Tohumeken

M.Sc. in Materials Science and Nanotechnology

Advisor: Ayşe Begüm Tekinay

Co-Advisor: Mustafa Özgür Güler

June 2016

Despite the fact that vaccination eradicates many diseases, a broad variety of disorders cannot be treated using current vaccine development methods. In addition, it is difficult to rapidly develop new vaccines following the sudden onset of a new pandemic, as the production and transport of vaccines to impoverished areas is still a major issue. The lack of sufficient vaccine production, for example, enabled the spread of swine flu in 2009, while HIV, Zika and malaria viruses currently lack effective vaccinations. In addition, while cancer vaccines represent a promising area of research, their clinical implementation is also limited by the absence of rapid and effective vaccine development methods. The development of new and effective vaccines is therefore quite vital. Moreover, recently used vaccines promote either humoral or cellular immune responses, while effective treatment requires the induction of both systems. Consequently, there is an urgent need for effective and easy-to-prepare vaccines that are capable of eliciting immune action through multiple channels.

Peptide amphiphiles are small molecules that are able to self-assemble into nanoscale fibrous networks. These nanofibers are biodegradable, biocompatible and do not

generate toxic byproducts, making them ideal for designing biomaterials. As such, nanofibers are a promising class of materials for inducing an effective immune response and overcoming some of the problems faced by current vaccine development methods.

In this thesis, I detail the use of biotinylated peptide nanofiber systems as immunomodulatory materials that are capable of incorporating a broad variety of antigens in a modular manner. Briefly, biotinylated and non-biotinylated peptide amphiphiles (PA) were first synthesized, purified and characterized to determine their material properties. PAs were then induced to self-assemble in the presence of CpG oligonucleotide (ODN) adjuvants, and ovalbumin was conjugated to self-assembled biotinylated-PA (B-PA) nanofibers by streptavidin linkers. Splenocytes were isolated from the mouse spleen and treated with bioactive nanofibers to investigate the effect of bioactive nanofibers on the immune response. Following the confirmation of an effective combined immune response, live mice were exposed to the nanofiber adjuvants as a proof-of-concept demonstration of *in vivo* PA-vaccine efficiency. Both *in vivo* and *in vitro* studies demonstrated that B-PA nanofibers are able to effectively modulate the immune response.

Given these observations, I suggest that the B-PA nanofiber can be used as an immunomodulatory material for promoting effective immune response against extracellular and intracellular pathogens, and especially for the vaccine-based treatment of cancer. As the antigen presented by the PA system can be changed in a modular manner, B-PA nanofibers can also be employed to rapidly develop new vaccines against sudden outbreaks of new viral strains.

Keywords: peptide amphiphile, self-assembly, nanofiber, adjuvant, Toll-like receptors, immune cell activation

ÖZET

İMMÜN CEVABIN DÜZENLENMESİ İÇİN BİYOTİNLENMİŞ PEPTİT NANOYAPILAR

Şehmus Tohumeken

Malzeme Bilimi ve Nanoteknoloji Programı, Yüksek Lisans

Tez Danışmanı: Ayşe Begüm Tekinay

Tez Eşdanışmanı: Mustafa Özgür Güler

Haziran 2016

Günümüz aşıları birçok hastalığı ortadan kaldırabildiği halde, bazı hastalıkların tedavisi için hala yetersiz kalmaktadır. Özellikle aniden yayılan hastalıklarda, aşının üretilme kapasitesi ve gerekli yerlere hızlıca nakil edilmesi, ya da nakil sırasında bozulmadan kalabilmesi sınırlıdır. Bu yüzden yeni aşıların geliştirilmesi hayati önem taşımaktadır. 2009 domuz gribi vakası sırasında, günümüz aşı sisteminde ne kadar eksiklik olduğu gün yüzüne çıkmıştır. HIV, malarya, zika gibi hastalık yapıcı patojenler için henüz etkili bir tedavi bulunamadığı gibi, kanserden ölen insanların sayısı da gün geçtikçe artmaktadır. Ayrıca, kullanılan çoğu aşılar, ya hücresel ya da humoral immün cevap oluşmasına neden olmaktadır. Etkili bir immun cevabın oluşması için hem hücresel hem de humoral immün cevabın etkili ve dengeli bir şekilde oluşması gerekmektedir. Bu yüzden yeni, etkili ve kolay hazırlanabilir bir aşı modelinin geliştirilmesine ihtiyaç duyulmaktadır.

Peptit amfifil denilen küçük moleküller, kendiliğinden bir araya gelip nano boyutlarda nanofiberler oluşturabilmektedir. Bu yapılar kolayca biyobozunabildiğinden, vücuda uyumlu olduğundan ve bozunduktan sonra zehirli ürün oluşturmadığından dolayı organizmalar için biyouyumluluk göstermekte ve uygulanabilir bir materyal olmaktadır. Bu yüzden bu yapılar, immünolojik cevabın etkin bir şekilde oluşturulması ve aşıların eksikliklerini kapatması için etkili bir yol olabilir.

Bu tezde, immün cevabın düzenlenmesi için kullanılan biyotinlenmiş peptit nanofiber sistemleri anlatılmaktadır. İlk olarak bu peptidin biyotinli ve biyotinsiz hali sentezlenmiş ve karakterize edilmiştir. Bir adjuvan olan CpG-oligonükleotid (ODN) ile karıştırılarak nanofiber yapılar oluşturulmuştur. Streptavidin bağlayıcısı kullanılarak model antijen olan ovalbumin, biotinli nanofibere bağlanmıştır. Daha sonra bu yapıların fareden alınan dalak hücrelerine etkisi ve farelere verildiğinde nasıl bir reaksiyon oluşturulduğu incelenmiştir. Bütün deneyler sonucunda, biyotinli nanofiberler immün hücreleri etkin ve düzenlenebilir bir immün cevap oluşturması için uyarmaktadır. Bu sonuçlar ışığında, biyotinli peptit nanofiberlerin etkili bir immün cevap tetikleyicisi olarak kullanılarak, hücre içi, hücreler arası patojenlere ve kansere karşı etkili bir çözüm sunabileceği kanısına varılmıştır. Kolay bir şekilde hazırlanabildiğinden ve taşıdığı antijeni ortaya çıkmış salgına göre ayarlanabileceğinden dolayı, bu sistem uygulanabilirlik açısından umut vadetmektedir.

Anahtar Kelimeler: peptit amfifil, kendiliğinden bir araya gelme, nanofiber, adjuvan, Toll benzeri reseptör, bağışıklık hücrelerinin aktivasyonu

Kuzenim Ali Durğun'a

(1989-2013)

ACKNOWLEDGEMENTS

I would like to express my appreciations to all people who contribute my MS thesis either by their experiences, knowledge, help or their mental and emotional support. I would like thank to my advisors, Prof. Tekinay and Prof. Güler for their guidance and support to my research. Their encouragement pushed me to perform at my best throughout my Master. They also contributed to my personal development and gave me a different perspective about social issues.

I would like to thank the National Nanotechnology Research Center (UNAM) and Bilkent University for providing pleasant facilities and required equipment. Bilkent University has been my home with all the unforgettable memories for the past eight years, including my undergraduate education I would like to thank to The Scientific and Technological Research Council of Turkey (TÜBİTAK) for BİDEB 2210 E master fellowship and TÜBİTAK grant number 114Z562.

I would like to indicate my greatest thanks and most sincere gratitude to my entire family's members. My father Aşem, my mother Halime, my brother İlhan, and my sisters Sevgül, Birgül who always believe in me and support me to become who I am now. My youngest brothers and sister deserves a lot more than acknowledgement for their emotional support. I have always felt the love and endless support of my family with me. They always show respect to my decisions and never turn their backs. They always encourage me and be with me when I feel hopeless to overcome struggles. I am proud of them and I feel very lucky to have such a family.

I would love to express my special thanks to Merve Tohumeken, my wife, my friend, my ewinamin and mother of Said Musa, our son. She was always with me and always support me either in good or bad times, her supports has been priceless. I am proud of her, because he is doing in both maternity and master. I would like to express my gratitude to The Kunt family for their support to my carrier and allowing me to get married with their daughter.

I would like to express my special thanks to our old PhD Dr. Rashad Mammadov and His wife Dr.Büşra Mammadov for sharing their knowledge, and valuable collaboration. I would like to express my special thanks to Nuray Gündüz, M. Burak

Demircan, Zeynep Orhan, Alper Devrim Özkan, Nurcan Haştar, Berna Şentürk, Fatih Yergöz, İdil Uyan and Merve Şen for their help in my hard time for their collaboration and friendship, which would not have been possible without their sincere efforts.

I would like to thank to Ahmet Emin Topal, Aref Khalily, Gökhan Günay, Elif Arslan, Özüm Sehnaz Günel, Çağla Eren, Yasin Tümtaş, Seher Yaylacı(Üstün) and Melike Sever for their sharing of lots of knowledge, experiences in AFM,CD, flow cytometer, microscopy etc. and for the fruitful scientific discussions and for their friendship.

I would also like to thank Gülistan Tansık, Dr. Ruslan Garifullah, Dr. Gülcihan Gülseren, Dr. Gözde Uzunallı, Meryem Hatip, Sever, Dr. Melis Şardan, Göksu Çinar, Mevhibe Yakut, Dr. Özlem Erol, Dr. Hakan Ceylan, Hatice Kübra Kara, Seren Hamsici, Egemen Deniz Eren, Oya İlke Şentürk, Begüm Kocatürk, Dr. Aslı Çelebioğlu, Zeynep Aytaç, Sude Selin Su Yirmibeşoğlu, Hepi Hari Susapto, İ. Ceren Garip, Dilek Sezer, İkra Gizem Yıldız, Elif Ergül, Aygül Zengin, Mustafa Beter, Canelif Yılmaz, Oğuz Tuncay, İbrahim Çelik, Özge Uysal, Zelal Yavuz, Ebru Şahin Kehribar, Ebuzer Kalyoncu, Aybegüm Samast, Kerem Emre Ercan and Tuğçe Önür for creating such a warm working environment.

I would like to thank to Mustafa Güler and Serhat, for technical assistance and helpful discussion. I especially thank to Suna Abla for spreading their happiness with her sincere smile. My special thanks to Zeynep Ergül Ülger and Zeynep Erdoğan for their technical help and friendship.

TABLE OF CONTENTS

TABLE OF CONTENTS viii

CHAPTER 1 1

1.1 Introduction 1

1.2 Self-assembled peptide nanostructures 2

1.3 An overview of the immune system 8

1.3.1 Innate immune system 9

1.3.2 Adaptive immune system 15

1.4 Toll like receptors and adjuvants 21

CHAPTER 2 30

2.1 Introduction 30

2.2 Experimental 34

2.2.1 Material 34

2.2.2 Peptide synthesis 34

2.2.3 Preparation of fiber nanostructures 35

2.2.4 Preparation of antigen bearing fiber nanostructures 35

2.2.5 Transmission electron microscopy (TEM) imaging 36

2.2.6 Atomic force microscopy (AFM) imaging 36

2.2.7 Circular dichroism (CD) spectroscopy 37

2.2.8 Polyacrylamide gel electrophoresis (PAGE) 37
2.2.9 Immunogold staining and transmission electron microscopy imaging .. 38
2.2.10 Binding assay by ELISA 39
2.2.11 Animals 40
2.2.12 Splenocyte culture and stimulation experiment 40
2.2.13 ELISA 41
2.2.14 The effect of nanostructures on cell viability 42
2.2.15 Staining of surface markers, SIINFEKL and flow cytometry 42
2.2.16 Evaluation of effects of PA/ODN nanofibers on immunized mice 43
2.2.17 Effects of PA/ODN nanostructure on splenocytes proliferation 43
2.2.18 Uptake of ODNs into splenocytes 44
2.3 Results and Discussion 45
2.3.1 Design and characterization of the PA/ODN nanostructure 45
2.3.2 Biotinylated ovalbumin binds to B-PA nanofibers 54
2.3.3 Nanofiber size and epitope density can be controlled by dilution and non-OVA binding peptide incorporation 56
2.3.4 B-PA/ODN nanostructure complex promotes cytokine secretion 60
2.3.5 PA/ODN nanofibers enhance expression of the maturation markers and cross-presentation of antigens and uptake of ODN 62
2.3.6 Effect of PA/ODN nanostructures on humoral immunity and splenocytes proliferation 66

CHAPTER 3 73

3. Conclusions and future perspectives 73

Bibliography 76

LIST OF FIGURES

Figure 1.1 A peptide amphiphile molecule structure...... 3

Figure 1.2 Fluorescent βtail fusion proteins stably integrate into self-assembling peptide nanofibers. 4

Figure 1.3 Enzymatic degradation profile of ODNs bound to self-assembled PA. 7

Figure 1.4 Haematopoietic stem cells differentiation...... 11

Figure 1.5 Relationship between innate immunity, adaptive immunity and invaders. 14

Figure 1.6 General mechanism of the adaptive immune responses after antigen recognition by antigen presenting cells. 18

Figure 1.7 CD4+ helper cells induce cells by secreting distinct but overlapping sets of cytokines...... 20

Figure 1.8 Simple demonstration of PRRs and PAMPs. 23

Figure 1.9 Pattern recognition receptors and their downstream pathways. 24

Figure 2.1 Chemical representation of PAs.……..……46

Figure 2.2 Characterization of K-PA. 47

Figure 2.3 Characterization of B-PA...... 48

Figure 2.4 Structural characterization of PA/ODN nanostructures. 49

Figure 2.5 Morphological characterization of PA/ODN nanostructures.51

Figure 2.6 Evaluation of K-PA/B-PA mixture on formation of self-assembled nanostructure with PAGE. 52

Figure 2.7 Cytotoxic effect of materials. 53

Figure 2.8 Antigen-bearing B-PA/ODN nanostructures. 55

Figure 2.9 Morphological characterizations of diluted self-assembled B-PA/ODN nanostructures...... 57

Figure 2.10 Control of antigen binding to PA/ODN nanostructure via ELISA...... 59

Figure 2.11 Cytokine secretion profile of splenocytes triggered by PA/ODN nanostructures and ODN. 61

Figure 2.12 Effect of PA/ODN and OVA on maturation marker of splenocytes. 63

Figure 2.13 *In vitro* stimulation of immune responses by PA/ODN and OVA...... 65

Figure 2.14 *In vivo* immunization with PA/ODN versus soluble antigen or antigen with ODN...... 67

Figure 2.15 IgG isotopes in sera of immunized mice with PA/ODN versus soluble antigen or antigen with ODN. 68

Figure 2.16 Splenocytes proliferation of immunized mice with PA/ODN versus soluble antigen or antigen with ODN. 70

Figure 2.17 Schematic illustration of B-PA nanofiber formation and associated transmission electron microscope images...... 71

Figure 2.18 Effect of PAs on the cellular uptake of FITC-ODN in dendritic cells. 72

LIST OF TABLES

Table 1-1 TLR recognition of microbial components 25

Table 1-2 Characteristics of the ideal adjuvants 27

Table 1-3 Major adjuvants and clinically approved adjuvants 27

Table 1-4 Adjuvants and their effect on immune system 29

LIST OF ABBREVIATION

PA	:	Peptide Amphiphile
AFM	:	Atomic Force Microscope
CD	:	Circular Dichroism
BrdU	:	Bromodeoxyuridine
FACS	:	Fluorescence Activated Cell Sorter
MHC	:	Major Histocompatibility Complex
ODN	:	Oligodeoxynucleotide
LC-MS	:	Liquid Chromatography Mass Spectroscopy
HPLC	:	High Pressure Liquid Chromatography
PAGE	:	Polyacrylamide Gel Electrophoresis
SEM	:	Scanning Electron Microscopy
TEM	:	Transmission Electron Microscopy
FBS	:	Fetal Bovine Serum
DMEM	:	Dulbecco's Modified Eagle Medium
TCP	:	Tissue Culture Plate
TLR	:	Toll Like Receptor
APC	:	Antigen Presenting Cell

CHAPTER 1

1.1 Introduction

Vaccination has been used as a preventive treatment for more than 200 years, and the eradication of smallpox and rinderpest stands as a testament to its impact in saving human and animal life. Nevertheless, the development of effective vaccines is still necessary due to the constant evolution of newer viral strains and transmission of zoonoses to human hosts. No vaccine has so far been successful against highly threatening diseases such as Zika, Ebola, HIV and malaria. In addition, new vaccine development methods may allow the selective targeting of cancer cells by the immune system, which would be of major importance due to the fact that cancer is expected to claim more than 11 million lives worldwide by 2030. Autoimmune diseases, neurodegenerative diseases and organ failures are other unsolved problems of the modern era, and vaccine development efforts may likewise assist in their treatment.

Rationally designed biomaterials allow us to solve a wide range of health problems. Recent developments in material science and biology have greatly broadened the scope of intelligent biomaterial design for therapeutic applications, since these materials can now be synthesized, functionalized, characterized, controlled and mass produced with considerable ease. Liposomes, self-assembled nanofibers, gold nanoparticles and other materials can now be synthesized and functionalized in the nanoscale with different sizes, and subsequently used for different purposes. Liposomes, for example, are commonly employed as drug delivery vesicles for cancer therapy. In this thesis, we have used self-assembled biotinylated peptide amphiphile nanofibers for tuning the

immune response against a specific antigen that is noncovalently attached to the peptide matrix.

1.2 Self-assembled peptide nanostructures

Self-assembed systems are prevalent in nature, and self-assembly is an attractive mechanism to construct materials exhibiting desired combinations of physical, chemical and biological properties. For example, the cell membrane is one of the best-known self-assembled structures. Self-assembled peptide nanostructures can be formed by mixing oppositely charged peptide amphiphiles (PAs) in aqueous environments [1-3]. PA molecules are mainly composed of hydrophilic and hydrophobic regions that are covalently bound. A typical PA includes four key regions as shown in Figure 1.1:

i) Hydrophobic domain: Generally formed by an alkyl tail

ii) β-sheet forming domain: Covalently binds to the alkyl tail and is composed of a short peptide sequence. This domain has the ability to form intermolecular hydrogen bonds.

iii) Charged domain: This domain is a versatile region. It enables PAs to be dissolved in water by providing charges, and is formed by either basic or acidic amino acids. Self-assembly can be controlled by neutralizing the charge of a PA with oppositely charged ions, pH change, an oppositely charged PA, or other materials such as ODNs.

iv) Bioactive domain: Similar to the charged domain this region is also a versatile region. This part can present bioactive epitopes, binding sites, differentiation signals etc. [3-7].

PAs can self-assemble into a range of novel nanostructures, which makes them attractive for various purposes in biomaterial engineering. Over the past decade, by changing the bioactive epitopes of PAs, a considerable number of studies have been performed for understanding the effects of PAs on biological systems, such as cell signal transduction, cell differentiation, cell adhesion in extra-cellular matrix (ECM), cell growth and cell mobility [3, 8].

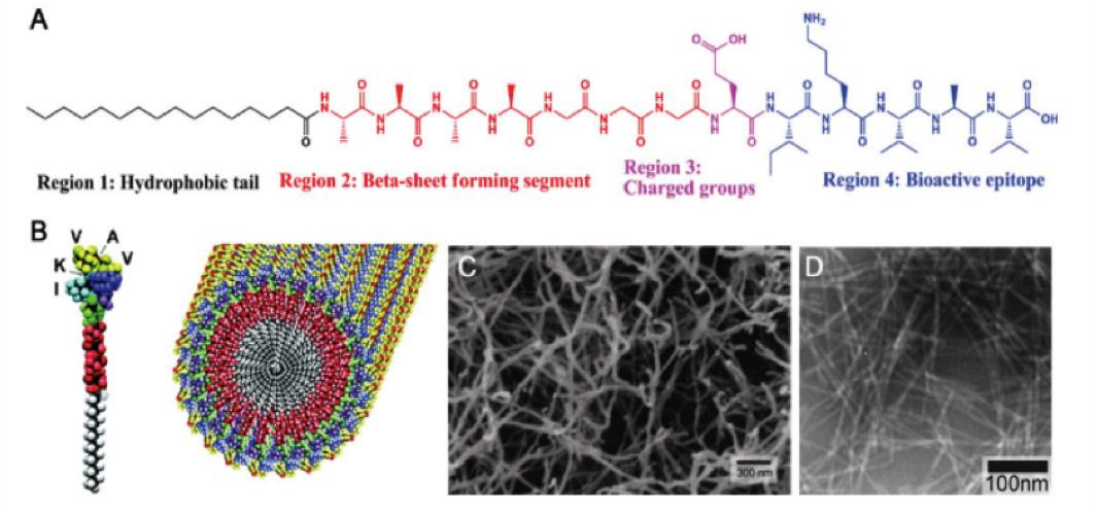

Figure 1.1 A peptide amphiphile molecule structure. A**)** Chemical structure of a PA molecule**.** B) Molecular demonstration of PA molecule and their self-assembled structure,(IKVAV was used as bioactive epitope). C) Scanning electron micrograph of the PA nanostructure in aqueous solution. D) Transmission electron micrograph of the PA nanostructure **(**Copyright © 2010 Wiley Periodicals, Inc. Reproduced with permission from [4]**)**

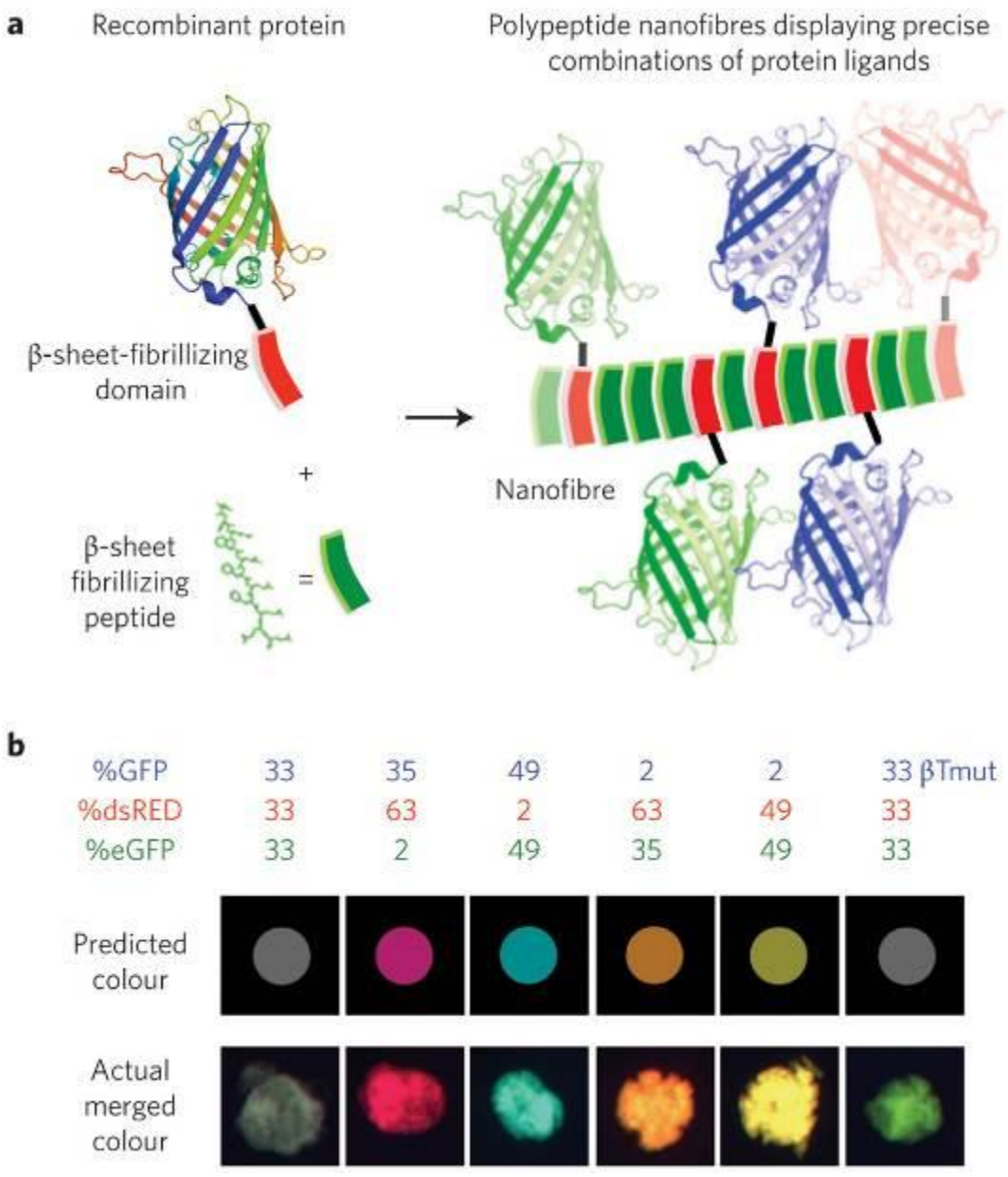

Figure 1.2 Fluorescent βtail fusion proteins stably integrate into self-assembling peptide nanofibers. a) A schematic representation of engineered fusion β-sheet fibrillating domain integrating into self-assembling peptide. **b)** Different fluorescent βTail proteins co-integrated into self-assembling peptide microgels at a different dose, and the correlation between actual gel colour and the predicted colour. (Green fluorescent protein, GFP; red fluorescent protein, dsRed; enhanced GFP, eGFP, mutated (βTmut)) (Copyright © 2010 NPG. Reproduced with permission from ref. [9])

Nanostructure formulation by peptide self-assembly is achieved through noncovalent interactions. Self-assembled peptides are commonly utilized in biomaterial research because of their ease of design, biocompatibility, defined functional motifs, fast response to the external environment, biodegradability, low immunogenicity as well as bioactivity [10, 11]. Active domains of self-assembled peptide nanofibers can also be designed for different purposes.

In one study, heparan-sulfate-mimicking PAs (HSM-PA) were synthesized and the effect of HSM-PA in combination with laminin-mimicking PAs on neurite outgrowth was analyzed. It was revealed that hydrogels made of self-assembling laminin-derived PA and HSM-PA increase the efficiency of neurite outgrowth compared to laminin-derived PAs alone. It was also shown that the scaffold in question is able to reduce the inhibitory effect of chondroitin sulfate proteoglycans (CSPGs), which makes it a promising therapeutic agent for central nervous system damages [12].

Another other commonly used bioactive epitope is IKVAV, which is a neurite-promoting laminin epitope that upregulates the proliferation of neural cells. Moreover, IKVAV reduces astrocyte formation and minimizes the risk of glial scars. In addition, it also prevents cells from undergoing apoptosis and mitigates astrogliosis. It was observed that self-assembling IKVAV-PA is more effective in modulating neuronal differentiation compared to laminin [13, 14].

In a series of interesting studies, Dr. Collier and coworkers approached self-assembled PAs in a different perspective. Instead of changing the active domain of PAs, they integrated β-sheet fibrillating domains into self-assembling peptides (Figure 1.2). This was accomplished by genetically synthesizing a GFP fusion β-sheet fibrillating

domain and mixing this protein with PAs. After characterization studies, they observed that PA bound to large proteins can nevertheless self-assemble into well-organized nanostructures [9]. Dr. Stupp and coworkers demonstrated a similar but harder approach for functionalized PAs. They first formed self-assembled peptide nanofibers and subsequently conjugated yellow fluorescent protein, cyan fluorescent protein or both to these self-assembled PA nanofibers using covalent linkage. Chemoselective native chemical ligation (NCL) reactions were utilized to synthesize such "hybrid" materials [15].

In recent studies, it was shown that PAs can be used for gene delivery as well [16, 17]. We have previously designed PAs that form nanostructures in the presence of CpG-ODN. We have shown that when ODN and PA/ODN nanostructures were treated with DNase1 enzyme, ODN alone gets degraded faster than the PA/ODN nanostructure (Figure 1.3). Additionally, it was shown that the PA/ODN nanostructure can prevent half of carried ODN from degradation for more than 24 h [18]. This system is very important for gene and adjuvant delivery systems, since effective delivery systems must protect their DNA or RNA cargo from endonucleases.

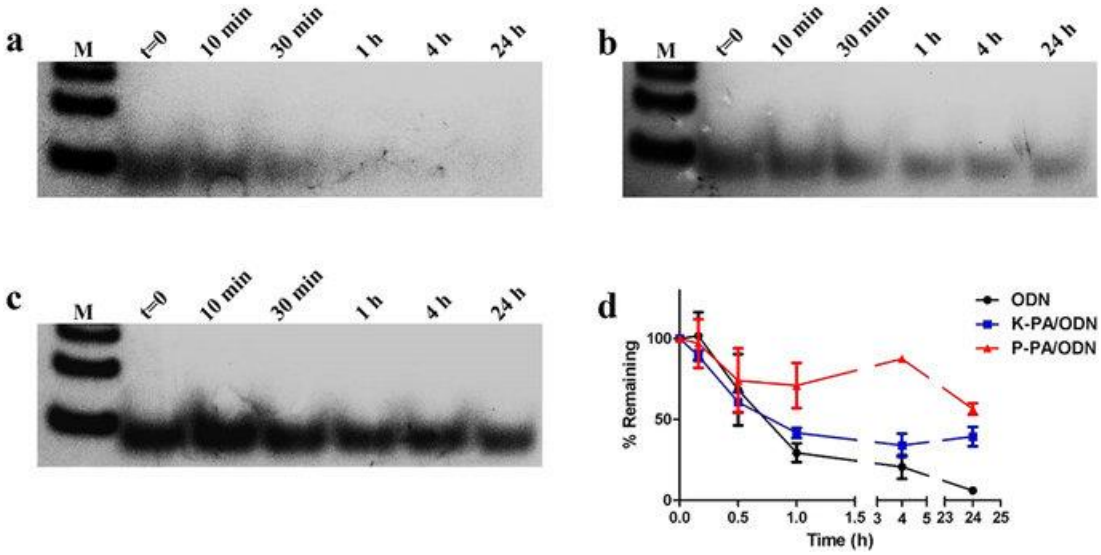

Figure 1.3 Enzymatic degradation profile of ODNs bound to self-assembled PA. (a) ODN alone, (b) nanofiber forming PA/ODN and (c) micell forming PA/ODN. Each group had been treated with DNAse I for different time periods. Remained ODN was analyzed by PAGE. Lane 1 is Marker, Lane 2 is non-treated ODN, Lane3-Lane7 = 10 min, 30 min, 1 h, 4 h and 24 h treatment with DNAse. (d) Graph of remaining ODN after degradation. Plotted according to calculated band intensities (Copyright © 2015 NPG. Reproduced with permission from ref. [18])

As a result, all information given from literature shows that rationally designed, self-assembled PAs serve as an interesting new tool for designing and developing powerful, controllable and functional materials for biological applications.

1.3 An overview of the immune system

Immunology was long known as the study of the body's defense against infection, but with the improvement in technology and diagnosis systems, it is found that immunology is not only the body's defense against infections but also body's defense against itself and other things. The foundation of immunology was laid in 1796 by Edward Jenner. He showed that inoculation with cowpox could prevent smallpox infection. He named this procedure as vaccination and this term is still used. Recently, vaccine are composed of weakened, inactivated or live-attenuated disease-causing agents. Basically, this strategy aims to teach immune cells about unknown diseases to be recognized by immune systems. Although, this strategy gave rise to successful results in eradication of some diseases such as smallpox, there is still some limitations. i) Effective vaccines are still not available in developing countries because of their high costs. ii) There is still no effective vaccine against HIV, malaria, zika viruses, tuberculosis and cancers. iii) Vaccine technology is old and not suitable for a rapid response to emerging outbreaks. For example, in the 2009 influenza A (H1N1) pandemic, it was concluded that there is limitation for producing more vaccine in short time, as well as distribution of them to other countries. iv) Traditional vaccines are produced by using live-attenuated viruses, inactivated viruses, attenuated bacteria or non-replicating recombinant viruses, however, there are safety concerns related to these vaccines. For instance, attenuated organism in the vaccine could gain virulent properties and cause disease.

To develop effective vaccines with minimum side effects, basic concepts in immunology should be taken into account.

1.3.1 Innate immune system

The innate immune system is the network of cellular and molecular elements that protect body from infections or diseases. The innate immune system responds to infection or damage rapidly and non-specifically. It is present at birth and is not gained after encountering infections, so it is not antigen specific [19]. The elements of the innate immune system include anatomical barriers, humoral molecules and cellular components.

Anatomical barriers are first innate immune system organs that infection agents encounter. It is composed of physical, chemical and biological barriers. Epithelial surfaces covering the skin, lungs and gut provide a physical barrier between the inside of the body and the invaders. The interior epithelial surfaces covered with a mucus layer prevented the entrance of microbial organisms into the body. Tight junctions between neighboring cells are other barriers that protect cells from potential pathogens. Movement of cilia or peristalsis protect air passages and the gastrointestinal tract from microorganisms. Tears and saliva including protective chemicals prevent infection of pathogens in the eyes and mouth. Fatty acids, lysozyme and phospholipase, which are abundantly found in the first line of immune system help clearing of microorganisms. Lysozyme and phospholipase are some of the material found in tears, saliva and nasal secretions. They can breakdown the cell walls of bacteria. Fatty acids in sweat, and some chemicals in stomach reduce pH of sweat and gastric secretions, preventing growth of bacteria. Gut and skin micro flora also help body to prevent colonization of microorganisms by secreting some toxic materials to other organisms or by competing them for nutrition [20]. When anatomical barriers are breached due to damages or

diseases, infection may occurs and humoral molecules are secreted for preventing infection. These humoral factors are complement systems proteins, cytokines, chemokines, acute-phase protein, interferons, interleukin1, lactoferrin and transferrin. Humoral factors play important roles in inflammation, recruitment of cells, promoting antibody formation, neutralizing viruses, attracting macrophages and neutrophils to a troubled spot, or killing bacteria directly [21]. Injured cells release specific chemical factors to stimulate inflammation. This mechanism generates a physical barrier to stop the spreading of infection, and also to promote healing of damaged tissues [22]. In response to tissue injury, a multifactorial network of chemical signals initiate a host response in the afflicted tissue. This response includes activation and migration of leukocytes (neutrophils, monocytes and eosinophils) from the venous system to the sites of damage [23]. Cellular barriers are formed after innate immune cells take their places. As shown in Figure 1.4, immune cells originated from hematopoietic stem cells. White blood cells (WBCs) which are also called leukocytes, make up 1% of total blood volume, and red blood cells constitute 40% to 50% of all blood volume. WBCs can be divided into two subgroups: granulocytes and agranulocytes [24]. Granulocytes are neutrophils, eosinophils, basophils, and mast cells; whereas agranulocytes are lymphocytes and monocytes. WBCs also can be separated into five main types: neutrophils, eosinophils, basophils, lymphocytes, and monocytes. Lymphocytes are composed of B cells, T cells and natural killer (NK) cells, and

monocytes include dendritic cell and macrophages. Additionally, dendritic cells, macrophages and neutrophils are known as phagocytic.

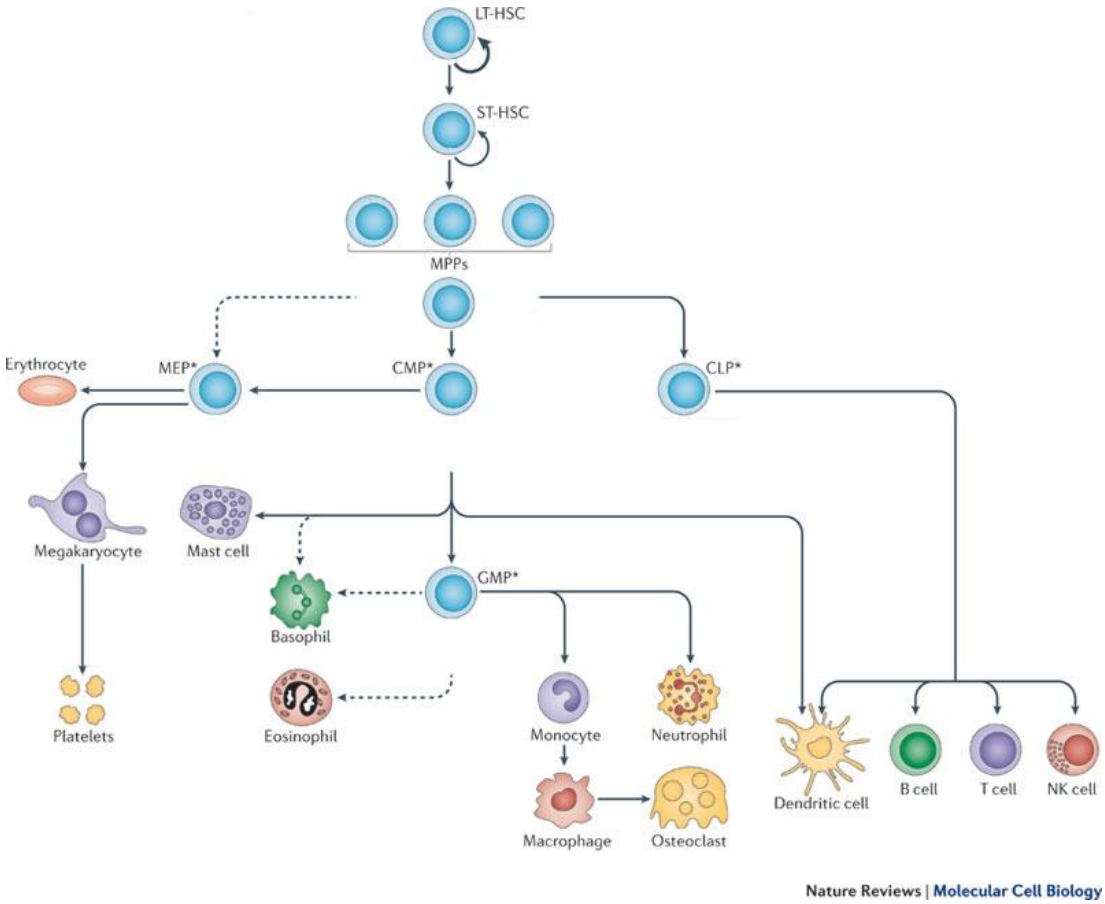

Figure 1.4 Haematopoietic stem cells differentiation. Haematopoietic stem cells (HSCs), are divided into at least two subsets: long-term reconstituting HSCs (LT-HSCs) and short-term reconstituting HSCs (ST-HSCs). LT-HSCs have self-renewal and multi-lineage differentiation potential throughout life. ST-HSCs have multipotency, but have more-limited self-renewal potential. Further differentiation of ST-HSCs generates multipotent progenitors (MPPs). Haematopoietic progenitor cells lose their differentiation potential in a stepwise fashion until they eventually generate all of the mature cells of the blood system. Lineage-committed oligopotent progenitors derived from MPPs include the common lymphoid progenitor (CLP), common myeloid progenitor (CMP), megakaryocyte-erythrocyte progenitor (MEP) and granulocyte-monocyte progenitor (GMP) populations. NK, natural killer. (Copyright © 2011 NPG. Reproduced with permission from ref.[25])

Innate immune cells include macrophages (MQ), dendritic cells (DC), neutrophils, basophils, eosinophils, mast cells and natural killer cells (NK). Each cell type in immune system has a different function. Neutrophils are specialized in engulfing microorganisms at infection sites. Basophils and eosinophils secrete toxic proteins and free radicals at the site of infection to kill parasites. Mast cells reside in connective tissues and mucosal membranes and take role in wound healing by releasing histamine and heparin. NK cells are quite special cells that can kill infected cells. Instead of engulfing pathogens, they are specialized in killing infected cells which do not express little expressions of self-antigens, which is a signal used to save normal cells from killing. Moreover, NK cells do not need further activation for killing any cells. Macrophages and dendritic cells are special cells that can take up pathogens, process, and present them to adaptive immune cells.

NK cells are responses to viral infections and tumor development. They are an important member of lymphocytes, their main function overlaps with T cells, however they take role in the first line of defense systems. NK cells were originally recognized by their ability to mediate lysis of certain susceptible tumor cell lines and infected cells. They have large granular lymphocyte morphology, but do not express T cell antigen receptors and the CD3 complex which are specific for T cells recognition. In addition, they can produce antimicrobial and immunoregulatory cytokines. These cells can secrete gamma interferon (IFNγ), tumor necrosis factor (TNF), and granulocyte/macrophage colony stimulation factor (GM-CSF). Their regulation can be controlled by innate cytokines which can mediate biological functions of NK cell

responses of cytotoxicity, proliferation, and interferon gamma (IFNγ) production [26-28].

Dendritic cells are also important cells of the innate immune system and they can be differentiated from common lymphoid progenitors and common myeloid progenitors. Dendritic cells can capture and process antigens, present antigen to adaptive immune cells, express lymphocyte co-stimulatory molecules, migrate to lymphoid organs and secrete cytokines to initiate immune responses. Moreover, besides activation of lymphocytes, they can also tolerate T cells to self-antigens, and other antigens, thereby minimizing autoimmune reactions. Like macrophages and B cells, dendritic cells are also known as antigen presenting cells (APC). They are efficient stimulators of B and T cells. After presenting antigens on their peptide-binding proteins, which are MHC class I and MHC class II, they stimulate cytotoxic T cells (CTLs) and helper T cells respectively. Without this engagement, T cells cannot be activated. They can produce IL-12, interferon and tumor necrosis factor alpha (TNF alpha) which have roles in T cell activation and activation of other immune cells. Therefore, these cells are powerful in manipulating the immune system. [29-31]

Monocytes are another class of innate immune system cells. They are the largest cells of the innate immune system. They become mature in bone marrow. They can circulate through the blood. Half of them are found in the spleen and the other half is located throughout the body. Monocytes differentiate into macrophages and dendritic cells. After crossing into tissue, monocytes differentiate into macrophages. They are very crucial for removing excess, damaged, or dead, and phagocytosis of bacteria, viruses and other pathogens. Macrophages express different types of pattern recognition

receptor (PRR) on their surface which are important for recognition of danger signal. Toll like receptor ones (TLRs) are the most important ones. When TLRs are activated by pathogens or other signals, this stimulates the macrophages to phagocytes pathogens or damaged cells. Additionally, it induces macrophages to secrete cytokines which can activate or recruit additional immune cells.

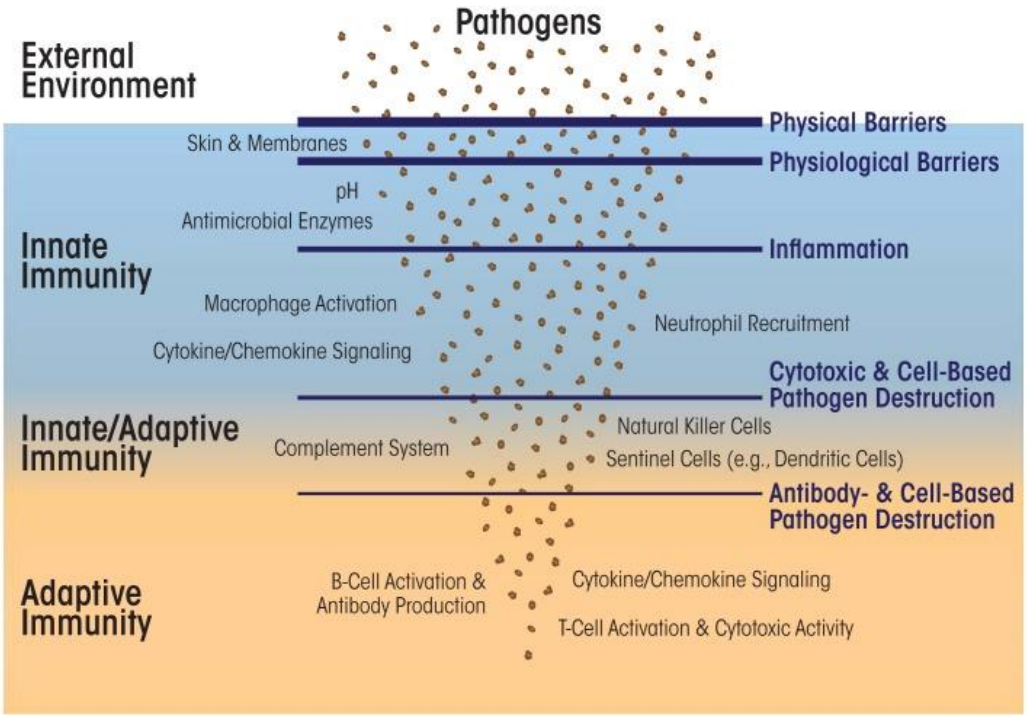

Figure 1.5 Relationship between innate immunity, adaptive immunity and invaders. Innate immunity consist of non-specific protective mechanisms against infection. The barriers including physical, physiological, chemical barriers, are cells and small proteins. The adaptive immune system comprises specialized cells and proteins. Several cells in adaptive immunity can store immune memory of a pathogenic invasion. The natural killer cells and dendritic cells have roles in both innate and adaptive immunity. (Copyright © 2015 ARCR. Reproduced with permission from Ref. [32])

Macrophages are members of antigen presenting cells, like B cells and dendritic cells. Another important role of macrophages is to induce inflammation. They are also known as scavenger cells in the body because they can clear dead cells and debris. Tumor necrosis factor α (TNFα) is mainly produced by macrophages. Macrophages also have important roles in healing process [32-34]. As it is shown in Figure1.5, innate immune system works as a supplementary system of adaptive immune system. They have common cells and also common cytokines which are important for regulating immune cell activity.

1.3.2 Adaptive immune system

Adaptive immune response, also called acquired immune response, is mediated by B and T cells. This system includes specialized cells and unique processes to eliminate pathogens from the body or prevent infections. It is acquired after birth. Adaptive immune cells are specialized to learn and remember, forming an immunological memory after encountering pathogens. The adaptive immune system is highly specific because the response is formed for specific antigens or toxins. If a patient is able to recover from an initial infection, they will not be affected by the same pathogen again, because adaptive immune response remains in reserve and responds quickly in the case of a second infection. Similar to the innate immune response, the adaptive immune response functions through antigen-specific humoral and cellular immune responses. T and B cells bear clonally-distributed antigen receptors. T-cell receptors (TCRs) and immunoglobulin are formed by somatic rearrangement. Once T cells are activated, they can directly attack infected cells, stimulate B cells to produce antibodies against pathogens, or enhance inflammation in the area of infection [35-37]. The somatic rearrangement of immunoglobulin is responsible for antibody production by B cells.

Activation of B cells by pathogens initiates a process of hypermutation in genes associated with the production of immunoglobulins, which increases the diversity of the resulting antibodies and increases the likelihood that one such protein will be specific against the antigen in question [38]. In some cases, B cells produce antibodies without undergoing hypermutation and secrete low-avidity antibodies [38].

T cells are specialized to eliminate cells infected with viruses, destroy detected cancer cells, or orchestrate the functions of innate and adaptive cells. T cells are further divided into different categories, including naive T cells (which further differentiate into T helpers and CTLs), memory T cells and regulatory T cells. An effective T cell-mediated immune response occurs after the activation of T lymphocytes by APCs in secondary lymphoid organs (the spleen, lymph nodes (LNs), Peyer's patches (PPs), tonsils, adenoids) [39].

Naive T cells are located in the thymus and differentiate from bone marrow. Following positive and negative clonal selection, they become mature non-effector cells that are individually specific towards a given antigen, but cannot recognize these antigens directly [40]. Helper T cells, known as CD4+ cells, are key elements of adaptive immunity. T helper cells can activate immune system cells, including B cells, killer T cells, and macrophages. Main T helper cells are Th1 and Th2. They serve as an important line of defense against intra- and extracellular pathogens and autoimmune and allergic responses. Th17 is a subgroup of CD4+ cells, and plays a role in chronic inflammation, autoimmune disease and the elimination of extracellular microorganisms. Regulatory T (Treg) cells are T cells that modulate the responses of effector T cells and suppress pro-inflammatory pathways. Due to this self-correcting mechanism, they also prevent immune cells from attacking normal body cells. T helper cells are activated by APCs, which express antigen fragments on their MHC class II molecules. This complex binds to T cell receptors (TCR) on T cells. Following this interaction, a second activation signal is provided through the effects of co-stimulatory molecules, which are either CD80 or CD86 on APCs. These co-stimulatory molecules bind to CD28 on T cells. A third signaling molecule, CD4+, then binds to MHC-CD80/CD86 complexes and enhances their binding affinity. Following MHC-TCR

binding, the helper T cell is activated and begins to proliferate. Activated helper T cells differentiate into Th1 or Th2 according to the milieu that T cells are found within. For example, IL-12 induces naïve T cells to differentiate into Th1 cells, while IL-4-stimulated cells form a Th2 response. In addition, Th1 cells produce IL-2, IFN-γ, TNF-α, and LT-α; while Th2 cells produce IL-4, IL-5, IL-6, IL-10, and IL-13. Some proliferating T cells may also become memory helper T cells. Those cells contribute to immunological memory and respond quickly when the body encounters the same pathogen again. The activated T cells are known as effector T cells, which release cytokines and induce apoptosis. Cytokines produced by T helper cells attract macrophages, B cells, and cytotoxic T cells, and/or regulate the activity of these cells [41-48].

Concentration of antigenic peptides, affinity of TCR toward the Ag/MHC complex, cytokines, inflammatory, and co-stimulatory signals in lymphoid organs affect the efficiency of T cell activation. CD8+ naive T cells differentiate into effector cytotoxic T lymphocytes (CTL) after encountering the above-mentioned requisite signals. As shown in Figure 1.6, CTL is activated after encountering an antigen segment presented on MHC I, and induces apoptosis. This mechanism is also important for clearing cancerous cells, which express tumorous antigens. Cluster of differentiation 28 (CD28) and cytotoxic T-lymphocyte-associated protein 4 (CTLA-4) are expressed on T cells. The ligation of CD28 with CD80/86 on APCs plays a co-stimulatory role for T cell activation, while the ligation of CTLA-4 with CD80/86 acts as a negative regulator. Conventional anticancer antibodies such as ipilimumab or tremelimumab were used to block the binding of CTLA-4 with CD80/86, suppressing the inactivation of T cells. The programmed death 1 (PD-1) inhibitory receptor is also expressed by T cells and negatively regulates their activity following its ligation with PD-L1 and PD-L2 [49-51].

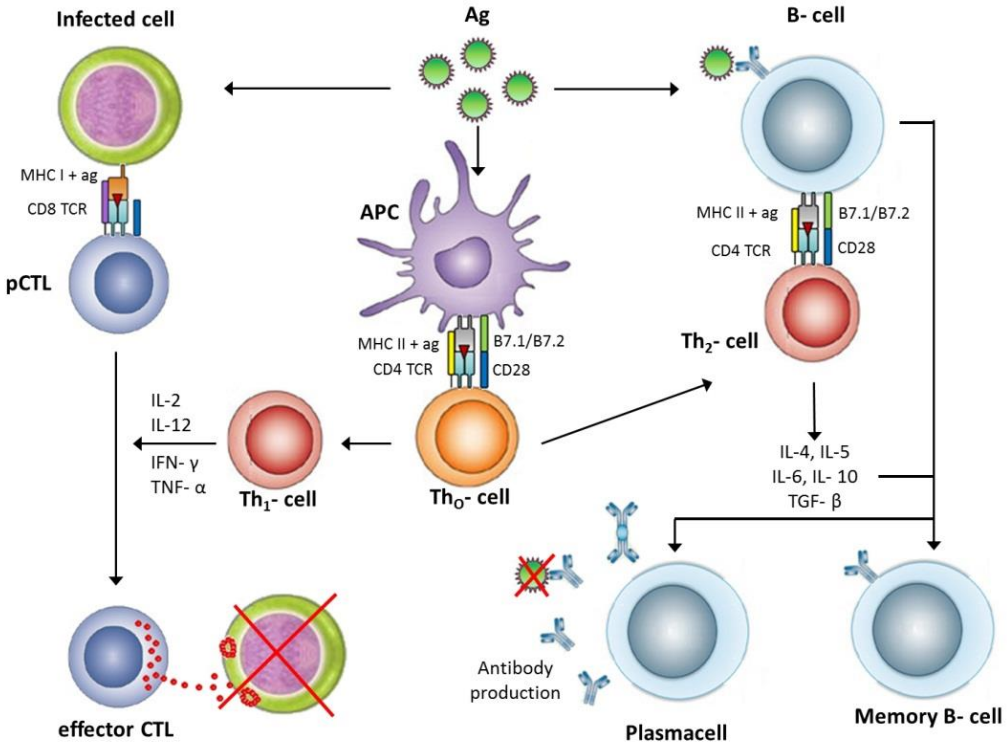

Figure 1.6 General mechanism of the adaptive immune responses after antigen recognition by antigen presenting cells. Antigens can be presented by either dendritic cells or B cells to T cells. APCs bearing the peptide-MHC I complex are recognized by precursor cytotoxic CD8+ T lymphocytes (CTLs). Moreover, infected cells can express pathogen specific antigens on their surface with MHC I or MHC II. Activated Th1 cells produce IL-2, IFN-γ, and TNF-α cytokines to induce activation and differentiation of the precursor CTLs into memory or effector CTLs. Effector CTLs can directly recognize and kill infected cells by the production of perforines and granzymes. Activated Th2 cells produce B cell stimulating cytokines such as IL-4, IL-5, IL-6, IL-10, TGF−β; which activate naive B cells. After activation, B cells differentiate into memory B cells and plasma cells that produce large amounts of IgG, IgA, IgE antibodies to prevent further virus infection. Ab: antibody, Ag: antigen, APC: Antigen Presenting Cell, DC: Dendritic Cell, IL: Interleukin, TCR: T Cell Receptor, Th: CD4+ T helper cell. **(**Copyright © 2012 Wiley Periodicals, Inc. Reproduced with permission from ref [47])

B cells are APCs and have the ability to recover antigens through their clonally formed antigen receptors, which are called membrane immunoglobulins (Ig). The B cell first recognizes antigens via its antigen receptor, and subsequently internalizes and degrades the antigen. After processing, antigens bound to MHC class II molecules are presented on the cell surface. Similar to other APCs, T cells recognize the processed antigens on the B cell surface and bind through the activity of TCR, CD4, CD40-L and/or CD28. CD40 is a co-stimulator expressed by B cells, and its interactions with CD40-L on T cells result in the differentiation and activation of B cells. Following binding, T helper cells recognize peptide fragments on MHC II molecules on the B-cells, allowing the activation of both cells against the same antigen. This interaction also triggers the expression of CD40-L on the T cell surface, which binds to CD40 on the B cell. This binding results in the stimulation of B cell clonal expansion, isotype switching, affinity maturation and differentiation into memory cells [52]. In addition to T cell-mediated activation, there is another B cell activation pathway that does not require T helper cells. This type of activation occurs in response to non-protein antigens such as polysaccharides, glycolipids, and nucleic acids. These antigens are not processed and presented along with MHC proteins, and cannot be recognized by helper T cells. Figure 1.7 shows that both Th1 and Th2 responses are able to activate B cells, and that cytokine exposure is able to determine the type of immunoglobulin secreted by the cells. Th1 helper cells preferentially induce B cells for IgG2a secretion, while Th2 helpers induce B cells for the synthesis of IgG1 and IgE [53]. Immunoglobulins are divided into five primary classes: IgG, IgM, IgA, IgD and IgE. The type of heavy chain in the molecule makes them distinguishable. IgGs are

abundantly found in serum: around 75% of serum IGs belong to subgroups such as IgG1 and IgG2a. IgG is the only antibody that can penetrate through the umbilical cord and impart passive immunity to the fetus.

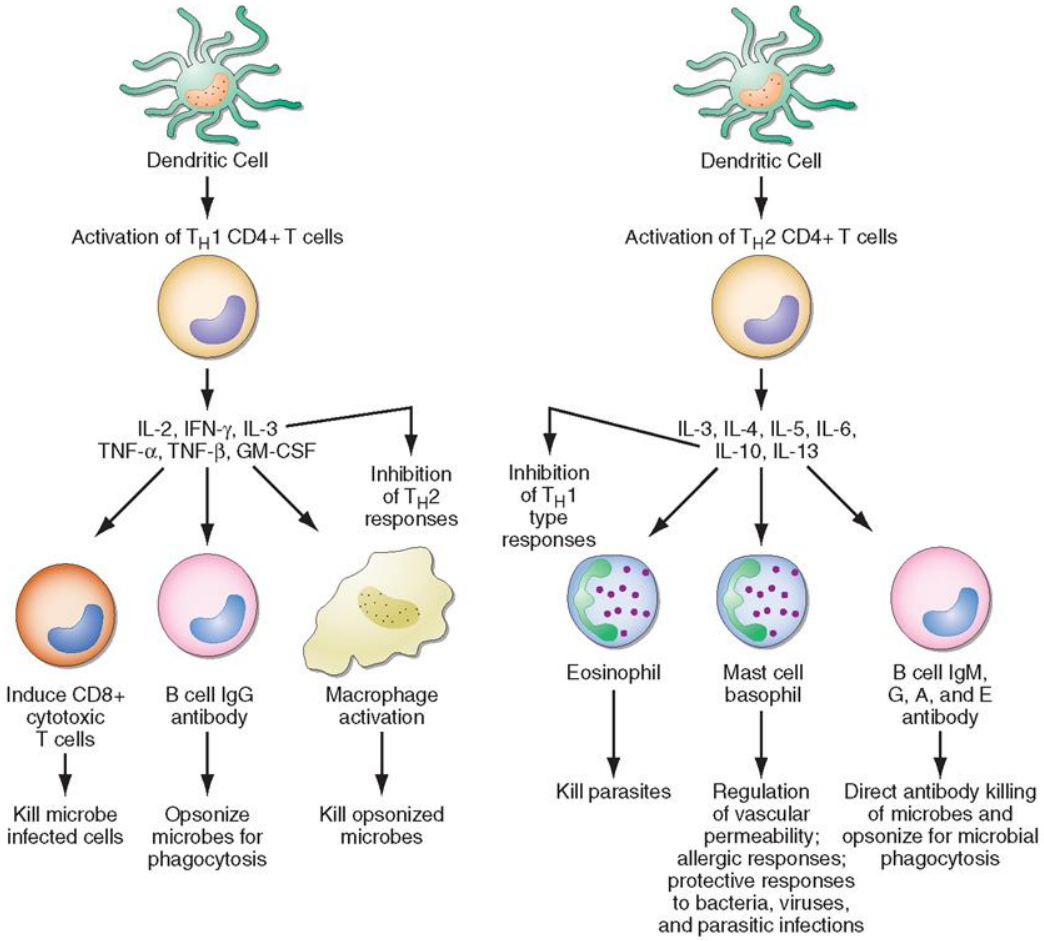

Figure 1.7 CD4+ helper cells induce cells by secreting distinct but overlapping sets of cytokines. T_H1 CD4+ cells activate immune cells for inflammatory and cellular reactions against intracellular bacteria or viruses. T_H2 CD4+ cells activate immune cells for specific types of antibody against parasites and extracellular encapsulated bacteria. T_H2 CD4+ cells play a role in allergic diseases. GM-CSF, granulocyte-macrophage colony stimulating factor; IFN, interferon; IL, interleukin; TNF, tumor necrosis factor. (Copyright © 2007 Elsevier, Reproduced with permission from ref [54])

1.4 Toll like receptors and adjuvants

Pattern-recognition receptors (PRRs) are innate immune system proteins that are used to recognize microorganisms or their characteristic antigens. They are encoded in the germline. PRRs recognize microbial components such as lipoteichoic acids, lipoarabinomannan (LAM), lipopolysaccharides (LPS), CpG-ODNs and lipoproteins. These components are known as pathogen-associated molecular patterns (PAMPs). PAMPs are essential for the survival of many microorganisms; consequently, the evolutionary pressures associated with their synthesis are too strict to drive their change, making them ideal targets for the innate immune system. For example, LPS are found in the cell wall of Gram-negative bacteria and protect them from chemical factors. PRRs are expressed constitutively in the host, allowing the recognition of pathogens at all stages of life. Different PRRs recognize specific PAMPs and activate specific signaling pathways, resulting in distinct anti-pathogen responses. For instance, LPS are recognized by Toll like receptor 4 (TLR4) and induce interferon secretions [35, 36]. PRRs are found on the surface of the cell membrane, within the endosome and in cytosol (Figure 1.8). Basic classes of PRRs are shown in Figure 1.8. However, these only represent a small part of the diversity exhibited by PRRs, because a broad range of PRRs are required to recognize common pathogens and pathogenic particles (Figure 1.9)

Toll like receptors are important members of PRRs. Toll was initially identified in *Drosophila*, and was demonstrated to be essential for the development of embryonic dorsoventral polarity in this organism [37]. Later, it was also shown to play a critical role in the antifungal response of flies [38]. To date, 12 members of Toll like receptors

have been identified. Macrophages, dendritic cells (DCs), B cells, specific types of T cells, fibroblasts and epithelial cells are known to express TLRs intracellularly or extracellularly. Environmental stresses and cytokines can affect the expression of TLRs. While TLRs 1, 2, 4, 5, and 6 are expressed on the cell surface, TLRs 3, 7, 8, and 9 are found in intracellular compartments such as endosomes. As shown in Figure 1.8, intracellular TLRs generally recognize bacterial DNA or viral RNA or DNA. As such, they are important for recognition of nucleotide sequences associated with intracellular pathogens [36, 39, 40].

TLR9 recognizes bacterial genomic DNA or virus DNA. Both bacterial and viral DNA are immunostimulants because of the presence of unmethylated CpG dinucleotide motifs [41]. Compared to mammalian genomes, bacterial genomes have a greater tendency to feature the unmethylated CpG motif. The methylated CpG motif, in contrast, is characteristic of vertebrate genomes and cannot activate mammalian immune cells. The presence of CpG-DNA can activate immune cells by upregulating the production of inflammatory cytokines that support the Th1 response. It was shown that synthetically designed DNA containing the CpG motif can induce immune cells in a manner comparable to bacterial DNA. TLR9 is found in the endosome, so bacterial DNA must first be delivered to this intracellular compartment prior to its recognition. Bacteria or viruses that are engulfed by the endosome are exposed to acidic and reducing conditions, which lead to the degradation of DNA into multiple single-

stranded CpG-motifs. After the degradation of envelope or coat of bacteria or viruses, TLR9 can interact with CpG-containing regions [42].

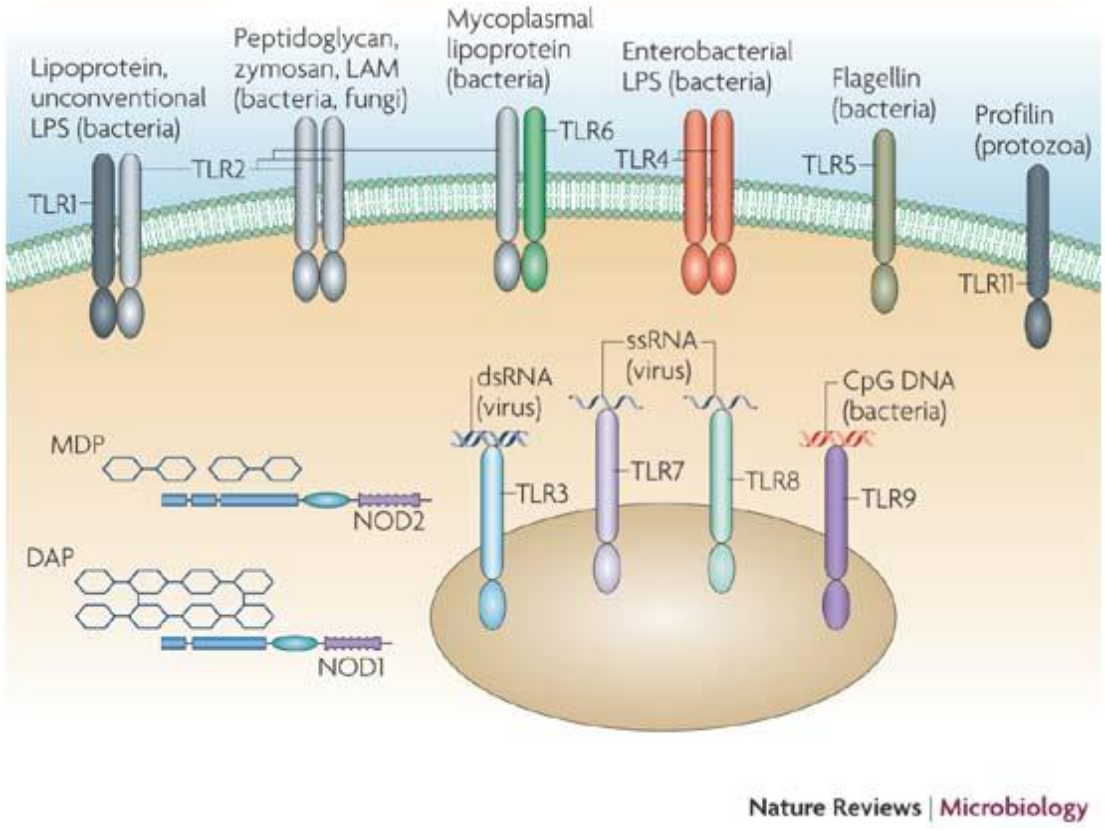

Figure 1.8 Simple demonstration of PRRs and PAMPs. Nod-like receptor (NLR) family. DAP, diaminopimelic acid; ds, double-stranded; MDP, muramyl dipeptide; LPS, lipopolysaccharides; LAM, lipoarabinomannan; ss, single-stranded. (Copyright © 2007 NPG. Reproduced with permission from ref.[43])

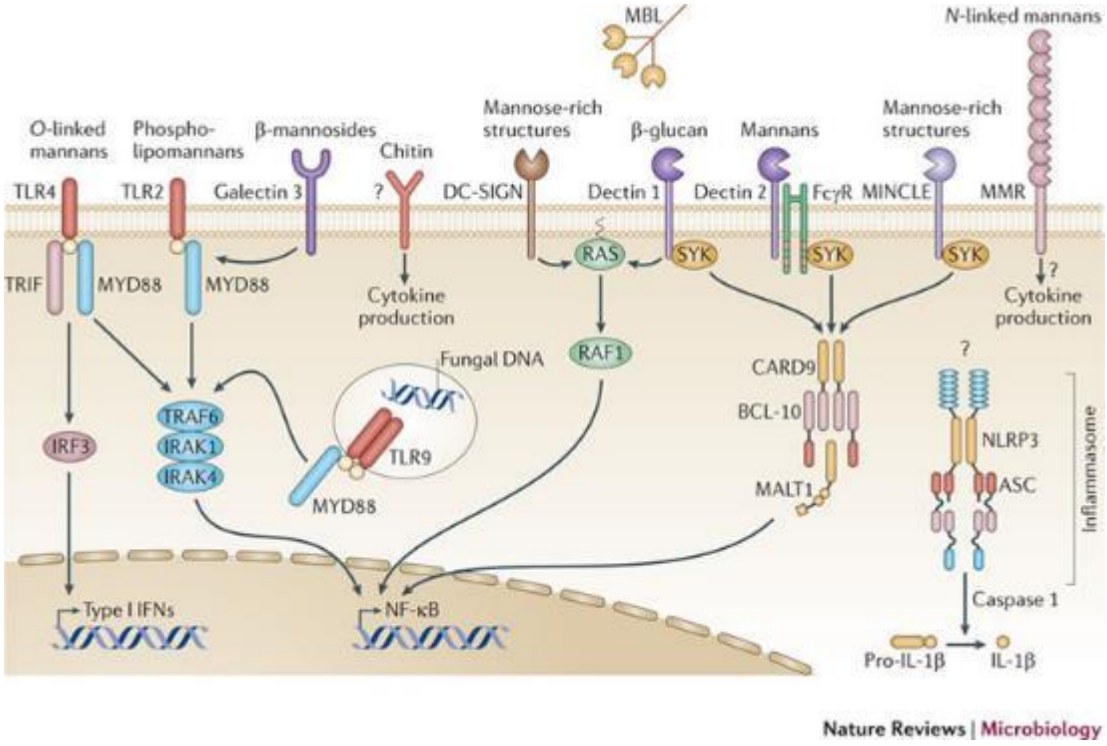

Figure 1.9 Pattern recognition receptors and their downstream pathways. The soluble lectin receptor mannose-binding lectin (MBL) can bind to mannose-rich structures. The membrane-bound C-type lectin receptors, macrophage mannose receptor 1 (MMR), dendritic cell-specific ICAM3-grabbing non-integrin (DC-SIGN) and macrophage-inducible C-type lectin (MINCLE) can recognize mannose-rich structures. Dectin 1 can recognize and bind to Î²-glucans, and dectin 2. Toll-like receptor 4 (TLR4) recognizes O-linked mannans, and TLR2 can recognize phospholipomannans or, together with galectin 3, recognizes Î²-mannosides. TLR9 is located in the cytosol and recognizes DNA. Furthermore, the NOD-like receptor (NOD-, LRR), apoptosis-associated speck (ASC). IFNs, interferons; IL-1Î², interleukin-1Î² and NF-ÎºB, nuclear factor-ÎºB also assist in the recognition process. (Copyright © 2007 NPG. Reproduced with permission from ref.[44])

Table 1-1 TLR recognition of microbial components (taken from ref. [36])

Microbial Components	Species	TLR Usage
Bacteria		
LPS	Gram-negative bacteria	TLR4
Diacyl lipopeptides	*Mycoplasma*	TLR6/TLR2
Triacyl lipopeptides	Bacteria and mycobacteria	TLR1/TLR2
LTA	Group B *Streptococcus*	TLR6/TLR2
PG	Gram-positive bacteria	TLR2
Porins	*Neisseria*	TLR2
Lipoarabinomannan	Mycobacteria	TLR2
Flagellin	Flagellated bacteria	TLR5
CpG-DNA	Bacteria and mycobacteria	TLR9
ND	Uropathogenic bacteria	TLR11
Fungus		
Zymosan	*Saccharomyces cerevisiae*	TLR6/TLR2
Phospholipomannan	*Candida albicans*	TLR2
Mannan	*Candida albicans*	TLR4
Parasites		
tGPI-mutin	*Trypanosoma*	TLR2
Glycoinositolphospholipids	*Trypanosoma*	TLR4
Hemozoin	*Plasmodium*	TLR9
Profilin-like molecule	*Toxoplasma gondii*	TLR11
Viruses		
DNA	Viruses	TLR9
dsRNA	Viruses	TLR3
ssRNA	RNA viruses	TLR7 and TLR8
Envelope proteins	RSV, MMTV	TLR4
Hemagglutinin protein	Measles virus	TLR2
ND	HCMV, HSV1	TLR2
Host		
Heat-shock protein 60, 70		TLR4
Fibrinogen		TLR4

ND = not determined. See text for references.

As demonstrated in Table 1-1, TLRs and their ligands may differ considerably between organisms. Additionally, particles that drive different types of TLR' immunity may

originate from the same organism. This mechanism enhances the recognition of pathogens by TLR.

Vaccination is an effective way to prevent infectious diseases. The main aim of vaccination is to induce a strong immune response to pathogen-derived antigens and provide long-term protection against infection. Purified or recombinant antigens exhibit poor immunogenicity and cannot raise a substantial immune response. Materials that are used to enhance the specific immune response against co-inoculated antigens are called adjuvants. The word adjuvant originates from the Latin word *adjuvare*, which means to help or to enhance. As previously mentioned, immune cells recognize organisms by binding to PAMPs through their PRRs. As such, the former category of molecules can be used as adjuvants. However, if they are not purified sufficiently, they can be toxic. Therefore, less toxic derivatives of PAMPs are particularly attractive as potential adjuvants. For example, bacterial components are often potent immune activators. Bacterial DNA sections including CpG motifs are one of the most potent cellular adjuvants. CpG motifs are unmethylated cytosine-guanine dinucleotide sequences that are found in bacterial DNA and are absent in the mammalian genome. The CpG motif is recognized by TLR9 and induces the proliferation, activation and differentiation of immune cells Additionally, it directs the immune response toward the Th1 pathway [45, 46].

Adjuvants are used for different purposes: to enhance the immunogenicity of highly purified or recombinant antigens; to reduce the amount of antigens used for immunization; to reduce the number of immunizations; to improve the efficacy of

vaccines in newborns, the elderly or immunocompromised persons; or to enhance the uptake of antigens by the mucosa [47, 48].

Table 1-2 Characteristics of the ideal adjuvants (taken from ref.[49])

1. It must be safe, including freedom from immediate and long-term side effects.
2. It should be biodegradable or easily removed from the body after its adjuvant effect is exhausted to decrease the risk of late adverse effects.
3. It should elicit a more robust protective or therapeutic immune response combined with the antigen than when the antigen is administered alone.
4. It must be defined chemically and biologically, so that there is no lot-to-lot variation in the manufactured product, thereby ensuring consistent responses in vaccinees between studies and over time.
5. Efficacy should be achieved using fewer doses and/or lower concentrations of the antigen.
6. It should be stable on the shelf to be commercially and clinically useful.
7. The adjuvant should be affordable.

Table 1-3 Major adjuvants and clinically approved adjuvants (taken from ref.[46])

Adjuvant	Major Immunostimulatory Component(s)	Innate Receptors or Pathway Activated	Principal Immune Responses Stimulated
Licensed Adjuvants			
Alum	aluminum salts	NLRP3 inflammasome (?)	Ab, Th2 (+ Th1 in humans)
MF59 and AS03	squalene-in-water emulsions	tissue inflammation (no receptors defined)	Ab, Th1 + Th2
AS04	MPL plus alum	TLR4 and inflammasome (?)	Ab, Th1
Adjuvants in Widespread Experimental Use or in Late Stage Clinical Development			
Poly-IC (also Poly-ICLC)	synthetic derivatives of dsRNA	TLR3, MDA5	Ab, Th1, $CD8^+$ T cells
MPL and formulations (AS01, AS02)	MPL and QS-21	TLR4 (MPL), ? (QS21)	Ab, Th1
Flagellin, flagellin-Ag fusion proteins	Flagellin from *S. typhimurium*	TLR5	Ab, Th1 + Th2
Imiquimods	imidazoquinoline derivatives	TLR7, TLR8 or both	Ab, Th1, $CD8^+$ T cells (when conjugated)
CpG oligodeoxynuceotides and formulations (IC31, QB10)	synthetic phophorothioate-linked DNA oligonucleotides with optimized CpG motifs	TLR9	Ab, Th1, $CD8^+$ T cells (when conjugated)
CAF01	trehalose dimycolate (cord factor)	Mincle	Ab, Th1, Th17
ISCOMS and ISCOMATRIX	saponins	mechanism undefined	Ab, Th1+ Th2, $CD8^+$ T cells
IFA (and Montanide formulations)	mineral or paraffin oil + surfactant	mechanism undefined	Ab, Th1 + Th2
CFA	IFA + peptidoglycan, trehalose dimycolate	NLR, inflammasome, Mincle, TLR?	Ab, Th1, Th17

The principal immune response stimulated is based on results from human and mouse studies, although it may be limited to one species in some cases. Where indicated, conjugation of TLR ligand to antigen is necessary to obtain significant $CD8^+$ T cell responses.

The biological pathways by which adjuvants perform their functions are subject to debate. However, there is some evidence that adjuvants may utilize a variety of mechanisms to elicit immune responses. These mechanisms include the depot effect (through which the adjuvant sustains the release of antigens at the site of injection); up-regulation of cytokines and chemokines; cellular recruitment at the site of injection; increasing antigen uptake of APCs and presentation of antigens; activation and maturation of APCs (*e.g.* by promoting the expression of MHC class I, MHC class II or co-stimulatory molecules); inducing APCs to migrate to the draining lymph nodes; and/or the activation of the inflammasome [50]. A great number of adjuvants have been characterized to date, but few have been approved by Food and Drug Administration (FDA) (Table1.3.3). Approved adjuvants are used for different treatments and can induce different immune responses, as shown in Table 1.3.4. Consequently, the choice and dose of adjuvants can be optimized to efficiently induce the immune system towards a desired response mechanism.

Table 1-4 Adjuvants and their effect on immune system (taken from ref.[50])

Adjuvants	Proposed mechanisms of action	Immune response activated	Licensed vaccines
Alum	No depot effect NLRP3 activation *in vivo*? Independent of TLR signaling ↑ Local cytokines and chemokines ↑ Cell recruitment (eosinophils, monocytes, macrophages) ↑ Ag presentation	↑ Ab responses ↑ Th2 responses Poor Th1 responses	Many human vaccines (e.g., DTap, Hib, Hepatitis A, Hepatitis B)
MF59	No depot effect NLRP3 independent but ASC-dependent Independent of TLR signaling but MyD88-dependent for Ab responses ↑ Local cytokines and chemokines ↑ Cell recruitment (neutrophils, macrophages, and monocytes) ↑ Ag uptake Activate muscle cells ↑ Ag-loaded neutrophils and monocytes in dLNs	Balanced Th1 and Th2 responses	Licensed for influenza vaccine (Fluad®), H5N1 pre-pandemic vaccine (Aflunov®), H1N1 pandemic vaccines (Focetria® and Celtura®)
AS04	MPL signals through TLR4 to activate APCs ↑ Local cytokines and chemokines ↑ Cell recruitment (DCs and monocytes) ↑ Ag-loaded DCs and monocytes in dLNs	↑ Ab responses ↑ Th1 responses	Licensed for human papilloma virus (HPV) (Cervarix™), hepatitis B virus (Fendrix®)
AS03	Spatio-temporal co-localization with Ag Transient ↑ cytokines locally and in dLNs ↑ Cell recruitment (granulocytes and monocytes) ↑ Ag-loaded monocytes in dLNs	↑ Ab responses ↑ Immune memory	Licensed for pandemic flu vaccine (Pandemrix®)
Virosomes	Ag delivery vehicle Bind APCs and induce receptor-mediated endocytosis Escape endosomal degradation Ag presentation via MHC class II and MHC class I to CD4+ T cells and CD8+ T cells respectively Immunopotentiator	↑ Ab responses ↑ CTL responses	Licensed for Inflexal® V and Invivac® influenza vaccine and hepatitis A vaccines (Epaxal®)

Ab, antibody; Ag, antigen; CTL, cytotoxic T lymphocytes; dLNs, draining lymph nodes.

CHAPTER 2

2.1 Introduction

Despite improvements in vaccine technology, effective vaccines have yet to be developed for diseases such as cancer, human immunodeficiency virus (HIV) infection, tuberculosis and malaria, which together cause the deaths of more than 4 million people worldwide each year [51, 52].Modern vaccines also require an extended development process, and cannot respond immediately to emerging outbreaks that follow the transmission of new viral strains from animal reservoirs to the human population [51]. For example, in the recent outbreak of Ebola and Zika viruses, it is reported that 13,562 people were infected by Ebola in West Africa [53] and 32,000 people were infected by Zika in French Polynesia [54]. It is also predicted that in 2030, cancers will claim the lives of more than 11 million people worldwide [55, 56]. Currently, clinically approved vaccine adjuvants such as aluminum hydroxide and the oil-in-water emulsion MF59 can promote humoral immune responses but not cellular immune responses [46, 57]. The activation of CD8+ T cells (CD8T) in particular is critical for the development of vaccines against cancer or intracellular pathogens such as human immunodeficiency virus (HIV), malaria and hepatitis C. As such, materials modulating humoral and cellular responses in a synchronized manner are preferred in vaccine development [58, 59]. Accordingly, inactivated virus-, live-attenuated virus- and viral vector-based subunit vaccines have been developed for inducing effective humoral and cellular responses [60]. However, these approaches have so far faced problems involving incomplete viral inactivation, regain of virulence and unfavorable host responses to viral vectors, which have limited their clinical utility [61].

Safety concerns associated with inactivated and live-attenuated virus vaccines have led to the development of recombinant protein-based subunit vaccines, which consist of one or more recombinant proteins or polysaccharides and do not utilize the active viral agent in any form. However, subunit vaccines induce poor or non-existent CD8T responses and exhibit low cross-presentation efficiencies, as they are not uptaken, processed and/or presented to naïve CD8T cells to the same extent as the entire viral unit [60-63]. The cross-presentation and immunogenicity of antigens can be improved through the administration of immunostimulatory molecules or adjuvants [64, 65], including aluminum, MF59, MPL, AS04, AS01B and AS02A, toll-like receptor (TLR) ligands, CpG-ODN1826, oil based adjuvants and other factors [49, 66-68]. In addition, antigens may also be delivered in particulate form in order to generate specific T cell responses, such as the Th1-type response [69]. Encapsulated or conjugated antigens have likewise been shown to induce greater humoral responses than soluble antigens [69-72]. To induce an effective immune response, adjuvant and antigens should be in close proximity [18]. The size of carrier materials is another important parameter for the generation of an effective immune response. Immunization with nanoparticles in the 200–600 nm range are known to induce higher levels of IFN-γ production, upregulation of MHC class I molecules and the production of antibody isotypes favoring the Th1-type immune response. Immunization with 2 – 8 μm microparticles, in contrast, enhance IL-4 secretion, upregulate MHC class II expression, and direct the immune response towards the Th2-type. On the other hand, nanoparticles in the 20−200 nm range can efficiently enter the lymphatic system through lymph drainage [73-75]. Previous studies have also shown that epitope density displayed on the

nanoparticles are crucial for effectively eliciting humoral immune responses, and especially the IgG response [76]. As such, materials to be used for antigen delivery applications should have controllable sizes and exhibit the ability to present epitopes efficiently to produce concerted T-cell responses. Highly effective T-cell vaccines fulfilling these criteria are still being sought, and a broad variety of methods have been employed for their development [63, 73]. As virus mimetic materials exhibit the potential to elicit strong immune responses while posing little to no health risks, we hypothesized that a rationally designed network of self-assembled peptide nanofibers can be used as an effective vaccine candidate to meet the stringent demands of the vaccine industry.

Self-assembly has been used as a powerful strategy for the construction of functional materials. Mediated by electrostatic forces rather than covalent binding, nanofiber formation by peptide self-assembly has attracted intensive research interest due to the ease of design, biocompatibility, defined functional motifs, fast response to external environment, biodegradability and low immunogenicity associated with these materials [11]. Self-assembled nanomaterial formation has been shown to exhibit immense potential for regenerative medicine, drug delivery, cell culture, analytical detection, biosensors and immunotherapy applications [4, 9, 77, 78]. Recently, Collier and co-workers have reported that self-assembling peptides can be used as powerful immune adjuvants [71, 79]. In another study, it was shown that peptide amphiphile (PA)-based micelles could serve as an effective antigen delivery system [77, 80]. Although the strategies developed by these groups are powerful and effective for vaccine production, they also suffer from limitations with regards to their synthesis

and assembly methods. The preparation of these materials involves the covalent conjugation of a protein or protein fragment to the self-assembling peptide, which is not readily applicable to all antigen fragments. However, the streptavidin (SA)-biotin system can be used in situations where direct covalent attachment is problematic, as it is known that the SA-biotin interaction is among the strongest non-covalent interactions in nature [81]. In a previous study, it was demonstrated that streptavidin binds strongly to biotinylated self-assembled nanostructures, and it was also shown that biotinylated insulin-like growth factor 1 (IGF-1) can bind to the peptide nanostructure through an SA linker [82].

In this work, we describe the development of a modular delivery system using a biotin-linked approach that allows a broad diversity of antigens to be presented on the surface of peptide nanofibers. Nanostructure formation by the ODN1826 adjuvant (a TLR9 agonist) [83] and biotinylated self-assembling peptides allowed highly specific binding of antigens to the nanostructure and positioned the antigens in close proximity with the adjuvant through the SA linker. We also demonstrate that the designed self-assembled (PAs/ODN+SA+OVA) nanostructure is able to induce humoral and cellular responses, and detail the mechanism of action of the adjuvant system using *in vitro* and *in vivo* models.

2.2 Experimental

2.2.1 Material

9-Fluorenylmethoxycarbonyl (Fmoc) and tert-butoxycarbonyl (Boc) protected amino acids, [4-[α-(20,40-dimethoxyphenyl) Fmoc-aminomethyl] phenoxy] acetamidonorleucyl-MBHA resin (Rink amide MBHA resin), and 2-(1H-benzotriazol-1-yl)-1,1,3,3-tetramethyluronium hexafluorophosphate (HBTU) were purchased from NovaBiochem and ABCR. Other chemicals for peptide synthesis were purchased from Fisher, Merck, AlfaAesar, or Aldrich. CpG ODNs were purchased from Invivogen. Paired antibodies and recombinant proteins of IFNγ and IL-12 were obtained from R&D systems, that of IL-6 from eBioscience. Reagents for polyacrylamide gel electrophoresis were obtained from Sigma Aldrich. Horseradish peroxidase-conjugated goat anti-mouse IgG (sigma), IgG1(eBioscience), IgG2a (abcam), or IgG2b (eBioscience) were obtained from Southern Biotechnologies (AL, USA). All cell culture and ELISA reagents were purchased from Life Technologies, except non-essential amino acid solution (Sigma Aldrich). Fluorescently labelled antibodies were obtained from eBioscience (CD40, CD86, Anti-Mouse OVA257-264 (SIINFEKL) peptide).

2.2.2 Peptide synthesis

Lauryl-VVAGK-Am (K-PA) and Lauryl- VVAGKK(Bio)-Am (B-PA) were synthesized on Rink Amide MBHA resin. Amino acid couplings were performed with 2 equivalents (equiv) of Fmoc-protected amino acid, 1.95 equiv of HBTU and 3 equiv of N,N-diisopropylethylamine (DIEA) for 2 h. After removal of Mtt group of Fmoc-

Lys(Mtt)-OH by %5 TFA solution in DCM, biotin was conjugated in the same manner as amino acid couplings. Removal of Fmoc group was achieved by 20% (v/v) piperidine in DMF for 20 minutes. To block the remaining free amine groups after amino acid coupling, 10% (v/v) acetic anhydride solution in DMF was used (30 min). After each step, the resin was washed using DMF, dichloromethane (DCM) and DMF. A trifluoroacetic acid (TFA)/triisopropyl silane (TIS)/ H_2O/DCM mixture (5:2.5:2.5:90 ratio) was used to cleave the peptide from the resins.

2.2.3 Preparation of fiber nanostructures

Fiber nanostructures were prepared through the self-assembly of peptide molecules in the presence of oligonucleotides. To form fiber nanostructure, positively charged K-PA and B-PA molecules were mixed with CpG (ODN1826), respectively. Sequence of ODN1826 is 5′ -tccatgacgttcctgacgtt-3′. The molar ratio for ensuring that all ODNs in solution interact with nanostructures was determined to be 100:1 for B-PA and K-PA/ODN as showed in our previous studies [84]. Nanostructures were prepared at these ratios for all experiments (K-PA/ODN) and (B-PA/ODN) throughout the experiments. In all experiments, at least three independent K-PA/ODN and B-PA/ODN formulations were prepared and tested.

2.2.4 Preparation of antigen bearing fiber nanostructures

Self-assembled B-PA/ODN and K-PA/ODN nanostructure were mixed with Streptavidin from Streptomyces avidinii (SA) (Sigma-Aldrich), and after 40 min, biotinylated ovalbumin (OVA) (Galab) was added to formed nanostructure. The exact

molar ratio for B-PA, Streptavidin and ovalbumin was 1:1:1. Antigen bearing nanostructure was formed.

2.2.5 Transmission electron microscopy (TEM) imaging

Nanostructures were imaged by TEM. 30 μL of PA/ODN complexes was prepared on parafilm by mixing 15 μL of 15 μg/mL ODN1826 with 15 μL of either 0.023% (w/v) B-PA (100:1 ratio) or 0.015% (w/v) K-PA (100:1 ratio). For PA-only samples, these concentrations of PAs were mixed with distilled water instead of ODN solution. For serial dilution, self-assembled B-PA/ ODN complexes were diluted (1 fold, 10 folds and 100 folds diluted). TEM grids were inverted onto these solutions. Grids were removed after 10 min and the remaining solution on grid was absorbed by a lint-free paper. Staining was performed with 2% (w/v) uranyl acetate solution (Ted Pella, Inc) for 40 seconds. Grids were washed with ddH_2O twice and dried 3 h at room temperature. TEM imaging was performed by a FEI Tecnai G2F30 instrument. All images were taken in STEM mode with a high angle annular dark field (HAADF) detector.

2.2.6 Atomic force microscopy (AFM) imaging

AFM imaging of PA/ODN complexes was performed in liquid conditions. ODN1826 solution at 15 μg/mL concentration was mixed with an identical volume of 0.023% (w/v) B-PA solution (100:1 ratio) or 0.015% (w/v) K-PA solution (100:1 ratio). The final ODN concentrations in each PA/ODN complexes were equal. For K-A/ODN complexes, the prepared solution was diluted 50 times, B-PA/ODN complexes was diluted 10 times, and dropped onto the cleaved mica surface and imaged directly in

aqueous environment (Figure 1D and F). Silicon nitride soft contact tip (BL-RC150VB, 37 kHz, k = 0.03 N/m) was used for contact mode imaging of K-PA/ODN complexes. Silicon tip (150 kHz, k = 5 N/m) was used for tapping mode imaging of B-PA/ODN complexes. MFP-3D Asylum microscope was used for imaging.

2.2.7 Circular dichroism (CD) spectroscopy

CD spectroscopy was performed with a JASCO J815 CD spectrometer at room temperature. 0.2 mM solutions of both K-PA and B-PA and their mixtures with ODN1826 (100:1) were measured from 300 to 190 nm. Scanning speed, data pitch, DIT and bandwidth were adjusted to 100 nm/min, 1 nm, 4 s and 1 nm respectively. All measurements were performed with three data accumulations and sensitivity was selected as standard.

2.2.8 Polyacrylamide gel electrophoresis (PAGE)

PAGE was performed to validate the critical ODN/PA ratio required to conjugate all ODNs in solution to PA nanostructures and observing effect of mixture of K-PA and B-PA on nanostructure formation. 1:100 molar ratio of ODN/K-PA was optimum ratio for nanostructure formation and charge neutralization [84]. 20 μg/mL ODN1826 solution (15 μL) was mixed with varying amounts of PA solutions (15 μL) to prepare different B-PA/K-PA ratios (from 1:1 to 1:10000). These solutions were mixed with Orange DNA loading dye (Fermentas) and loaded onto 20% polyacrylamide gels. 10 μL of 10 bp DNA ladder (O'range rulerTM, Fermentas) was used as marker. Gels were run at 75 V for 1 h and subsequently at 50 V for 2.5 h (in 1x TAE). Stains-all dye working solution (0.005%, w/v) was prepared freshly from stock solution (0.1% w/v)

as recommended by the manufacturer (Sigma Aldrich). Gels were incubated in Stains-all overnight (dark conditions and room temperature). On the next day, the destaining of gels was performed under sunlight and images were taken by a Nikon camera.

2.2.9 Immunogold staining and transmission electron microscopy imaging

Ovalbumin's binding to B-PA/ODN nanostructures was demonstrated by immunogold staining and TEM imaging. 30 μL of PA/ODN complexes was prepared on parafilm by mixing 15 μL of 15 μg/mL ODN1826 with 15 μL of either 0.023% (w/v) B-PA (100:1 ratio). TEM grids were inverted onto these solutions. Grids were removed after 10 min and the remaining solution on grid was absorbed by a lint-free paper. Grids were reversed onto 30 μL of blocking solution (Assay buffer, Invitrogen) and incubated for 2 h at room temperature. Drops on grids were absorbed, and SA (5.15 ng/mL in double-distilled water (ddH_2O)) was added onto the grids. After 1 h of incubation, grids were washed five times with ddH_2O. Drops on grids were absorbed, and OVA (68.9 ng/mL in ddH_2O) was added onto the grids and incubated for 1 h at room temperature (RT). Primary antibody (0.25 μg/mL, abcam) against mouse OVA was added onto grids and incubated overnight at 4 °C. Grids were washed with ddH_2O 5 times. Gold-conjugated antibody (25 nm gold particles conjugated to antimouse IgG), 1/20 diluted from stock with assay buffer, was put onto paraffin film, and grids were reversed onto this solution. After 1 h, grids were washed five times with ddH_2O. After drying at room temperature for at least 3 h, TEM (FEI, Tecnai G2 F30) imaging was performed. All images were taken in STEM mode with an HAADF (high angle annular dark field) detector.

2.2.10 Binding assay by ELISA

ELISA technique was performed to demonstrate the binding of OVA to B-PA/ODN nanostructure. MaxiSorp plates (Thermo Scientific, NUNC) were coated with serial diluted (2 fold) self-assembled PA nanofibers or with PA/ODN that changed antigen-binding site density by mixing K-PA with B-PA and blank solution overnight at 4 °C. PA/ODN nanostructure was formed by mixing 20 μL of 15 μg/mL ODN1826 with 20 μL of either 0.023% (w/v) B-PA (100:1 ratio), 0.015% (w/v) K-PA (100:1 ratio) or B-PA/K-PA mixture. The next day, the solutions were removed and the wells were washed with washing buffer (Tween 20 in 0.9% (w/v) NaCl solution, pH = 7.4). These plates exhibit high-affinity binding to PA nanofibers [85]. On the next day, plates were washed, dried by tapping and blocked with 0.5% BSA (2 h), incubated 1 h with SA (5.15 ng/mL in double-distilled water (ddH_2O)), OVA (68.9 ng/mL in ddH_2O) . Plates were washed 5 times with washing buffer and dried by tapping between each consecutive steps. Primary antibody (0.25 μg/mL, Abcam) against mouse OVA was added. Plate was incubated overnight at 4 °C. On the next day, plates were washed 5 times with washing buffer and dried by tapping and adding IgG-HRP (horse radish peroxidase)-conjugated IgG (2 h), consecutively, at room temperature. Plates were washed 5 times with washing buffer and dried by tapping in between. TMB (3,3′,5,5′-Tetramethylbenzidine) substrate was added at the last step and reaction was stopped after 30 min by 1.8 N H_2SO_4. Colour formation was measured by microplate reader (Spectramax M5, Molecular Devices) as absorbance at 450 nm wavelength. In order to obtain exact absorbance values solely to dye color, the value

was subtracted from a reference value (650 nm). All treatments were performed with at least three replicates and shown as mean +/− standard deviation.

2.2.11 Animals

All experimental procedures involving animals were approved and performed according to by the Animal Ethics Committee of Gazi University Hospital (Protocol G.Ü.ET-15.063). Primary spleen cells were obtained from adult BALB/c and C57BL/6 (10–14 weeks old) mice, which were maintained under controlled conditions and fed *ad libitum*.

2.2.12 Splenocyte culture and stimulation experiment

Spleens were removed and single cells were dissociated from bulk tissue by using the end of a syringe in culture media (2% FBS in RPMI-1640). Single cell suspension was collected carefully to exclude tissue debris. Cell suspension was centrifuged at 800 g for 10 min. Supernatant was discarded and cell pellet was resuspended in 1 mL red blood cells lysis buffer (10x RBC lysis buffer: 0.155 M NH_4Cl; 0.01M $KHCO_3$; 0.1mM EDTA dissolved in one liter of ddH_2O and diluted to 1x RBC lysis buffer). Then, 9 mL of RPMI-1640 with 5% FBS was added and centrifuged at 800 g for 10 min (these steps was performed three times). Cells were adjusted to 2×10^6 cells/mL cell density and cultured in 96-well plates as 200 μL/well (5×10^5 cells/well). The medium used for the splenocyte culture was composed of RPMI-1640 with 5% FBS (Pen/Strep, L-Glu, non-essential amino acids and HEPES (20 mM) were also added). Cell stimulation was performed immediately after distributing cells to wells. PA/ODN nanostructures were prepared as described previously. Nanostructure and ODN-only

solutions were further diluted with media and final concentration of ODN in cell suspension was 1 μg/mL. For cytokine analysis, cells were cultured at 37 °C and 5% CO_2 for 48 h and supernatants were collected at the end of the experiment. For the analysis of surface markers (co-stimulatory molecules), SIINFEKL presenting cells were treated with same formulations for 24 h. Cells were collected at the end of the experiment for further staining and analysis by flow cytometry. All experiments were performed in triplicate; representative results of three independent experiments are shown.

2.2.13 ELISA

Effect of PA/ODN nanostructures on splenocytes were checked by measuring cytokine concentrations in supernatants collected from stimulation experiment with ELISA. MaxiSorpTM plates (Thermo Scientific, NUNC) were coated with IL-6, IL-12 or IFN-γ primary antibodies (overnight incubation at 4 °C). The next day, plates were blocked with 0.5% BSA (2 h), incubated with supernatants of cell culture experiment or standard recombinant proteins (24 h), biotin-labeled secondary antibody (2 h) and HRP (horse radish peroxidase)-conjugated streptavidin (1 h), consecutively, at room temperature. Plates were washed 5 times with washing buffer and dried by tapping between each consecutive steps. TMB substrate was added at the last step and reaction was stopped after 15–20 min by adding 1.8 N H_2SO_4. Color formation was measured by microplate reader (Spectramax M5, Molecular Devices) as absorbance at 450 nm wavelength (with a reference value at 650 nm). All treatments were performed with at least three replicates and shown as mean + /− standard deviation.

2.2.14 The effect of nanostructures on cell viability

The cytotoxicity of PA, ODN, and OVA was determined by analyzing the viability of wild type mouse embryonic fibroblast (wt-MEF) with live/dead and alamar blue assay. MEF cells were seeded in 96-well plates at a concentration of 5 x 10^3 cells per well for 24 h. After 24 h of incubation, 10 % Alamar blue (Invitrogen) solution was added to each well and incubated at 37 °C for another 4 h. The absorbance of each well at 450 nm (with reference wavelength of 620 nm) was measured by microplate reader (Spectramax M5, Molecular Devices). The results were expressed as cell viability percentage relative to untreated cells. For live/dead assay, 2 μM Calcein AM and 4 μM Ethidium homodimer-1(EthD-1) was mixed in 10 mL 1x PBS and plates were treated with this mixture for 30 min. Images were taken with inverted fluorescent microscope (Zeiss AxioObserver A1). The cytotoxicity assay was performed three times and the average value of the three measurements was taken.

2.2.15 Staining of surface markers, SIINFEKL and flow cytometry

For analysis of the expression of co-stimulatory molecules and SIINFEKL presentation, cells were stained with CD40 and CD86 and SIINFEKL antibodies. Treated cells were collected and washed with 1x PBS, centrifuged and resuspended in FACS buffer (3% BSA+ 1% sodium azide in 1x PBS). Flow cytometry was performed with Accuri C6-Cytometer- equipment with BD Accuri C6 Software. The number of events was at least 20,000 for all samples. The experiment was performed in triplicate and representative results of two independent experiments are shown.

2.2.16 Evaluation of effects of PA/ODN nanofibers on immunized mice

For *in vivo* immune evaluation, male 10–14 weeks old Balb/c mice were administered with 500 μL vaccine formulations subcutaneously (s.c.). 4 groups (n = 5) of animals were treated with Ova (antigen) alone, Ova with CpG ODN, Ova with K-PA/CpG ODN or Ova with B-PA/ ODN (all in isotonic sucrose solution). 10 μg Ova was given to all animals, while CpG ODN amounts were 10 μg in relevant groups. Booster injections were performed at day 15. At days 13 and 28, animals were bled, and sera were obtained. IgG amounts in sera were detected with ELISA. Ova antigen was coated onto 96-well plates, blocked with 1% BSA buffer and serially diluted (10 fold) sera were added onto the wells. IgG was detected with HRP conjugated anti-IgG. Absorbance in each well was measured after substrate (TMB) addition. For splenocyte proliferation, animals were sacrificed at days 21 and 28 and spleens were removed for analyzing splenocyte proliferation. Single cells were dissociated from bulk tissue and 5×10^5 splenocytes were seeded to 96 well plates and then BrdU assay was performed.

2.2.17 Effects of PA/ODN nanostructure on splenocytes proliferation

Proliferation of cells after OVA stimulation was assessed using BrdU assay (Roche). Cells were seeded into wells at a density of 5×10^5 cells/well. Cells were incubated in standard cell culture medium supplemented with 10 μM BrdU labeling solution for 24 h. At the end of the incubation, BrdU incorporation assay was performed according to the manufacturer's instructions. Briefly, cells were fixed with FixDenat for 30 min and anti BrdU-POD solution was added into wells. Following 90 min of incubation and

tapping, substrate solution was added into wells and proliferation rates of the cells were quantified by measuring the absorbance (370 nm, with 492 nm reference wavelength) with microplate reader.

2.2.18 Uptake of ODNs into splenocytes

Internalization of ODNs and PA/ODN nanostructures into antigen presenting cells (APCs) which were freshly isolated from spleen, was analyzed by flow cytometry. For this purpose, FITC-conjugated ODN was used for preparing K-PA/ODN and B-PA/ODN. Mouse splenocytes were seed in 96-well plates (5×10^5 cells/well). Cells were treated with K-PA/ODN, B-PA/ODN or ODN alone, or each group with OVA were incubated for 2 h or 12 h before flow cytometry experiment. Cells were collected into 1.5 mL Eppendorf tubes by pipetting, and centrifuged. Supernatants were discarded, cells were washed with 1x PBS and a cell pellet was obtained again by centrifugation for further staining with specific antibody and analysis by flow cytometry.

All procedures regarding animals were approved by the Institutional Animal Care and Use Committee of Gazi University, Ankara, Turkey. This study was carried out in accordance with the approved guidelines.

2.3 Results and Discussion

2.3.1 Design and characterization of the PA/ODN nanostructure

Peptide amphiphiles (K-PA and B-PA) were synthesized and used in the production of self-assembled PA/ODN nanostructures (Figure 2.3.1.1). The lauryl group conjugated to peptide sequences drives their self-assembly through hydrophobic collapse in aqueous solutions. Glycine was used as a spacer, and lysine residues were included to provide a positive charge to PAs at physiological pH. In addition, the Val-Val-Ala peptide sequence was used to facilitate β-sheet formation by peptide molecules during self-assembly. Two lysine residues were utilized in the synthesis of B-PA; one lysine was utilized to graft biotin to the peptide backbone while the second lysine was used to impart a positive charge to B-PA, which enhances its solubility in aqueous media. This configuration splits the self-assembled peptide amphiphile into two functional regions; a hydrophobic inner core (consisting of an alkyl tail and β-sheet forming residues) and a hydrophilic outer shell (consisting of bioactive amino acids) [84, 86, 87]. A second layer of organization is provided through the interaction of positively charged K-PA and B-PA molecules (Figure 2.1) with negatively charged ODNs through electrostatic interactions, which allows the formation of cylindrical nanostructures. K-PA or B-PA was mixed with ODN to induce nanofiber formation. Characterization of material was performed afterwards.

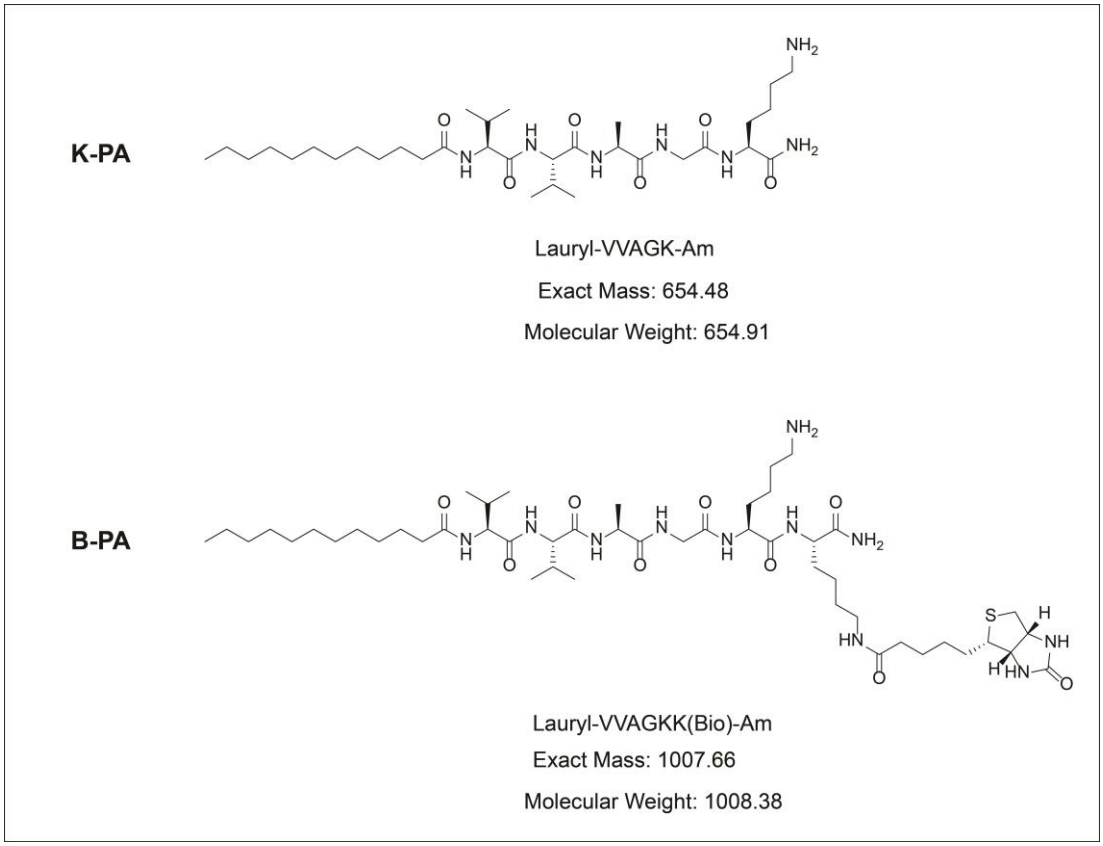

Figure 2.1 Chemical representation of PAs. Exact masses of K-PA and B-PA are 654.48 and 1007.66, respectively.

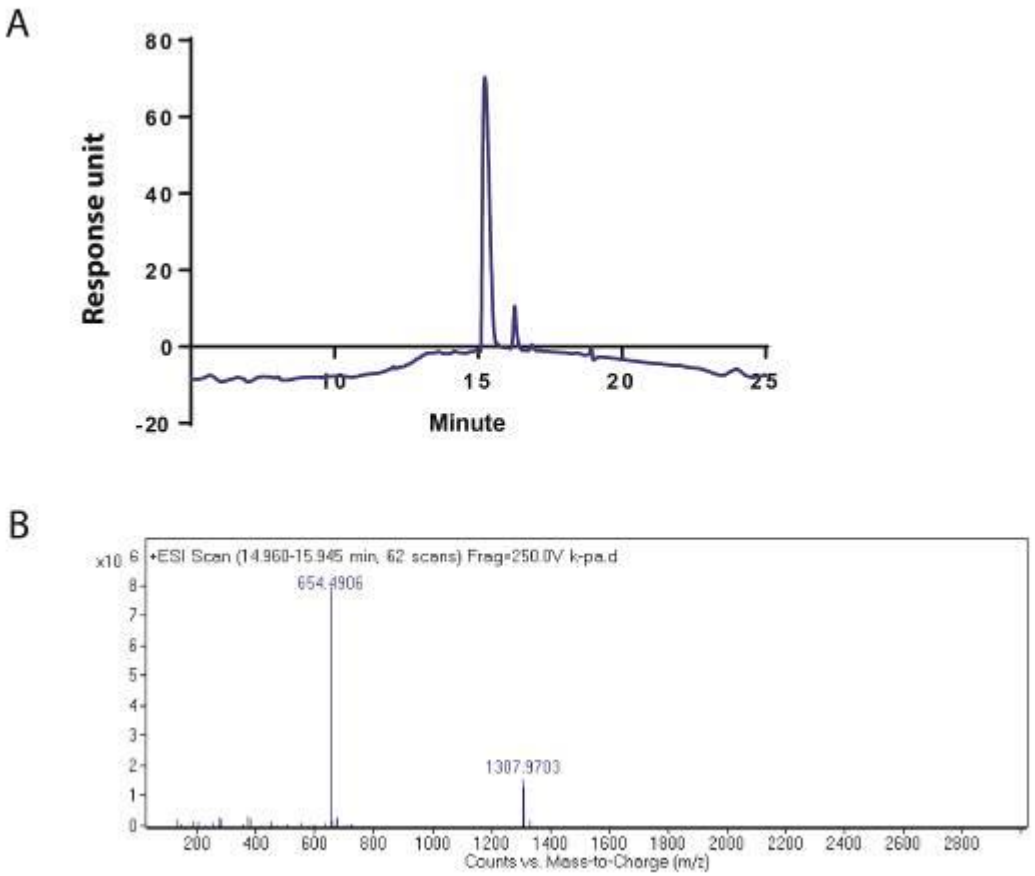

Figure 2.2 Characterization of K-PA. (A) LC chromatogram of K-PA molecule at 220 nm. (B) Mass spectrometry analysis of K-PA. $[M+H]^+$ (calculated) = 653.48, $[M+H]^+$(observed) = 654.49

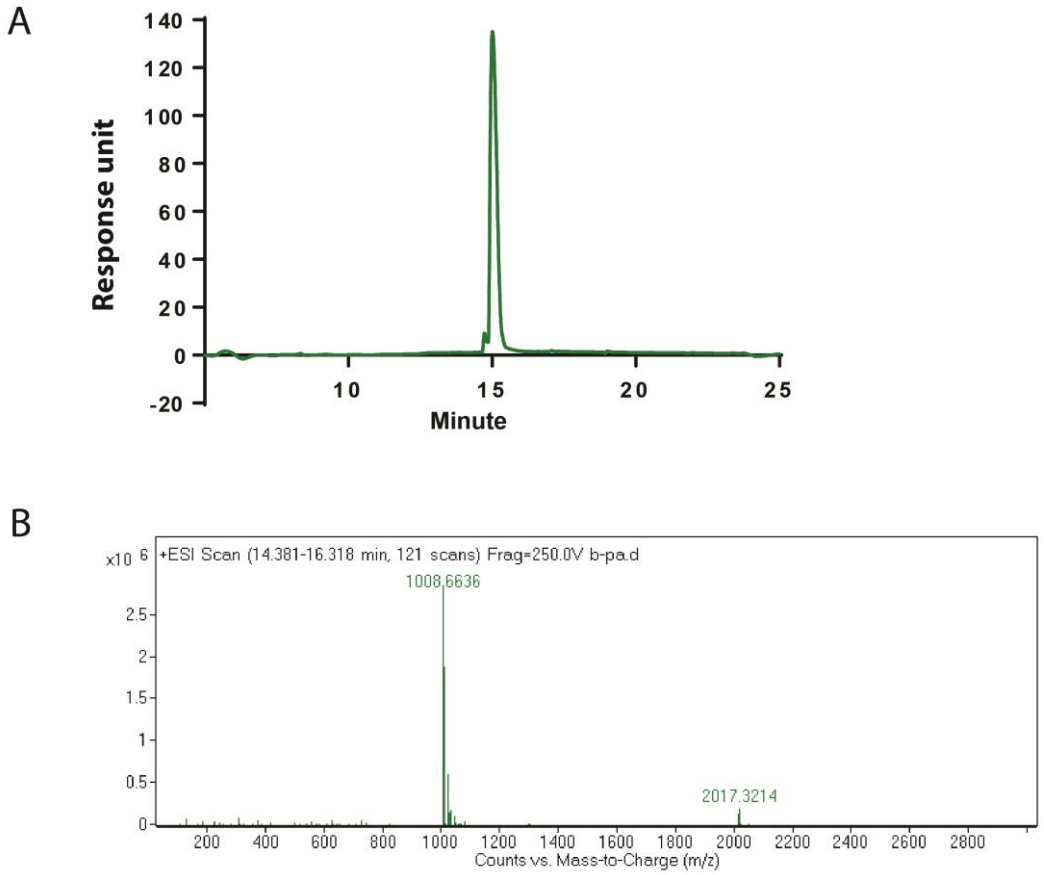

Figure 2.3 Characterization of B-PA. (A) LC chromatogram of B-PA molecule at 220 nm. (B) Mass spectrometry analysis of B-PA. $[M+H]^+$ (calculated) = 1008.38, $[M+H]^+$ (observed) = 1008.66

The synthesized PA molecules were purified with high performance liquid chromatography (HPLC) and analyzed with liquid chromatography-mass spectrometry (LC-MS). Chemical presentations of PAs are shown in figure 2.2 and their LC-MS results are shown in figure 2.1 and 2.3. The results indicated that PAs are highly pure and consistent with the expected masses. The secondary structures of PA and PA/ODN mixtures were investigated with circular dichroism (CD). CD spectra of both K-PA and B-PA were indicative of β-sheet formation, exhibiting a negative peak

at 217 nm and a positive peak at 197 nm. Similar results were observed following the mixing of ODN with B-PA or K-PA, while no peak was present in the ODN-only sample (Figure 2.4). CD results confirmed that K-PA and B-PA form β-sheets and that ODNs did not interrupt β-sheet formation.

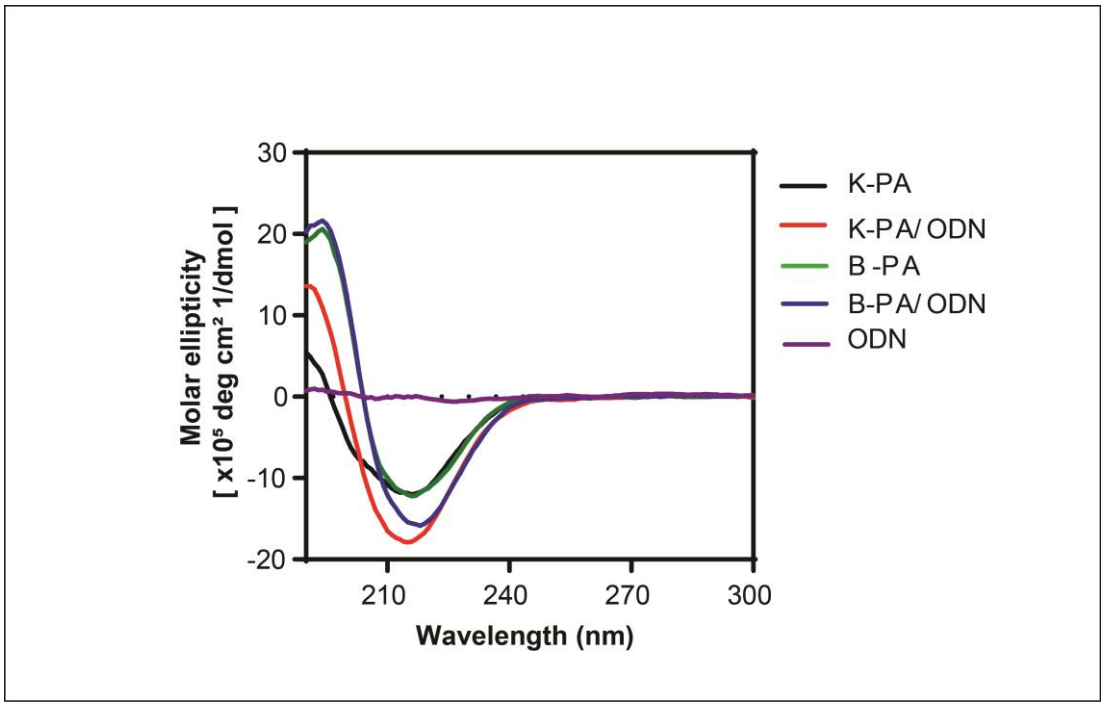

Figure 2.4 Structural characterization of PA/ODN nanostructures. CD spectra of ODN, PAs and PA/ODN complexes.

TEM and AFM images were taken to observe the morphology of K-PA/ODN and B-PA/ODN nanostructures in both dried and aqueous environments. TEM and AFM results show that K-PA and B-PA molecules formed cylindrical morphologies in the presence of ODN (Figure 2.5 C-E). The presence of ODN appears to enhance the complete self-assembly process.

AFM imaging of the PA/ODN complexes were performed to analyze the self-assembled systems in an aqueous environment. AFM was also performed to eliminate the effects of drying on the B-PA/ODN nanostructure formation. The K-PA/ODN and B-PA/ODN complexes showed cylindrical morphologies and were complementary to STEM images (Figure 2.5 D and F). In the aqueous environment, K-PA/ODN complexes were generally found to self-assemble into cylindrical bundles, while B-PA/ODN mostly assembled into small cylindrical complexes. These aggregation morphologies, taken in conjunction with the cylindrical structures formed by PA/ODNs on AFM images, underlines the dynamic nature of peptide/ODN assemblies and the complex-dependent self-assembly tendency of the peptides.

In order to conjugate all ODNs in solution into nanostructures, positively-charged PAs and the negatively-charged ODN were mixed in pre-optimized ratios for the self-assembly process. In our previous study, we demonstrated that the K-PA/ODN mixture is able to form nanofiber structures at a 100:1 molar ratio of PA-to-ODN, as supported by zeta potential and polyacrylamide gel electrophoresis (PAGE) measurements. To observe whether that ratio could also be used for B-PA, PAGE was performed with different molar ratios of K-PA/ B-PA with ODN (K-PA/B-PA+ODN). Our PAGE analyses suggest that 100:1 B-PA/ODN was a suitable ratio for nanostructure formation (Figure 2.6 B). Consequently, 100:1 ratio of B-PA/ODN was used for sample preparation in TEM and AFM imaging. K-PA/B-PA mixtures were also found to exhibit similar nanofiber structures as their components, allowing K-PA to be used

as a spacer for biotin in “mixed” nanofibers containing both PA sequences (Figure 2.6. A and B).

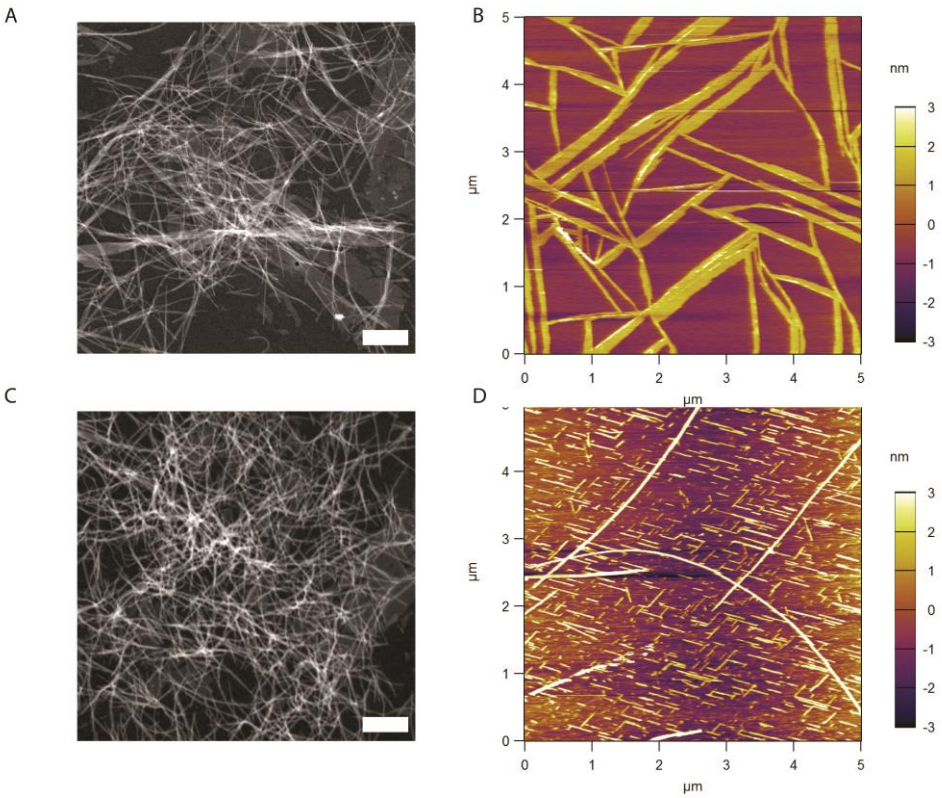

Figure 2.5 Morphological characterization of PA/ODN nanostructures. (A) STEM images of the K-PA/ODN nanostructure. Scale bar is 100 nm. (B) AFM images of K-PA/ODN nanostructure in aqueous environment. (C) STEM images of the B-PA/ODN nanostructure. Scale bar is 100 nm. (D) AFM images of the B-PA/ODN nanostructure in aqueous environment.

.

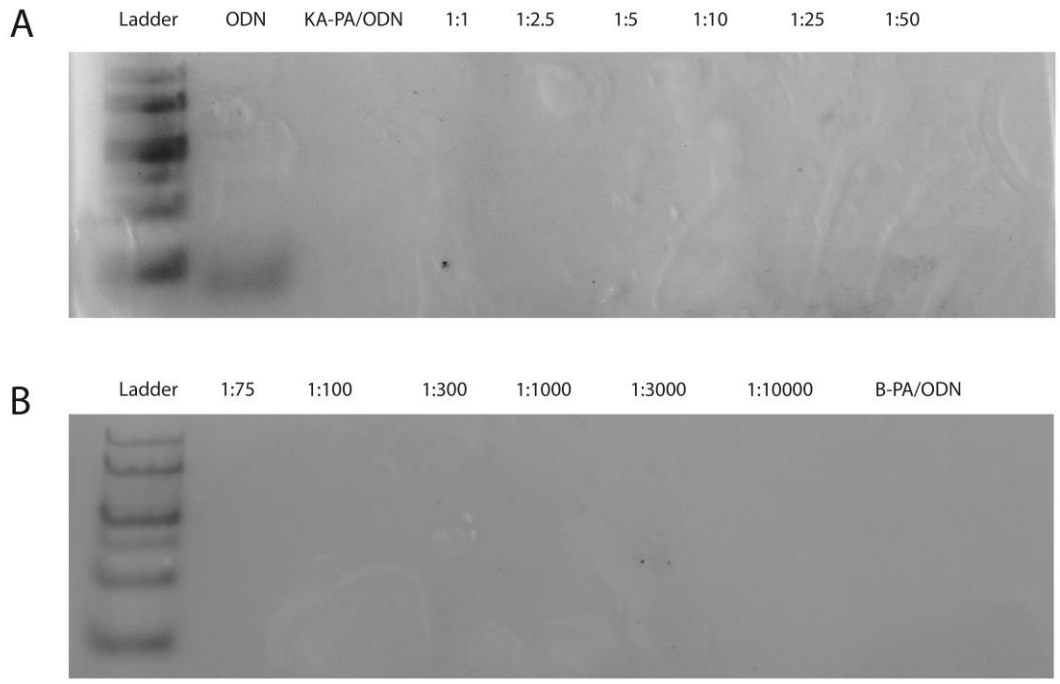

Figure 2.6 Evaluation of K-PA/B-PA mixture on formation of self-assembled nanostructure with PAGE. A) PAGE of only ODN, K-PA/ODN (100:1 Molar ratio), and B-PA-K-PA mixture with ODN (B-PA/K-PA radios are given as molar ratio and mixture with ODN as final ratio of PA/ODN (100:1)). B) PAGE of B-PA/ODN (100:1 molar ratio), and B-PA-K-PA mixture with ODN (B-PA/K-PA radios are given as molar ratio and their mixture with ODN as final ratio of PA/ODN (100:1)).

The biocompatibility of PA, ODN, and OVA were determined by Live/Dead and Alamar Blue assays. Wild type mouse embryonic fibroblast (wt-MEF) have been used for viability analyses. MEF cells were treated with the materials for 24 h. After 24 h of incubation, Live/Dead and Alamar Blue assays were performed. MEF cells were employed for assessing the skin irritation potentials of the material. The skin irritation can induce immune responses, so unexpected results can be observed when the

material are used for in vivo experiments. Therefore, to overcome such problems, viability analysis was performed with MEF cells.

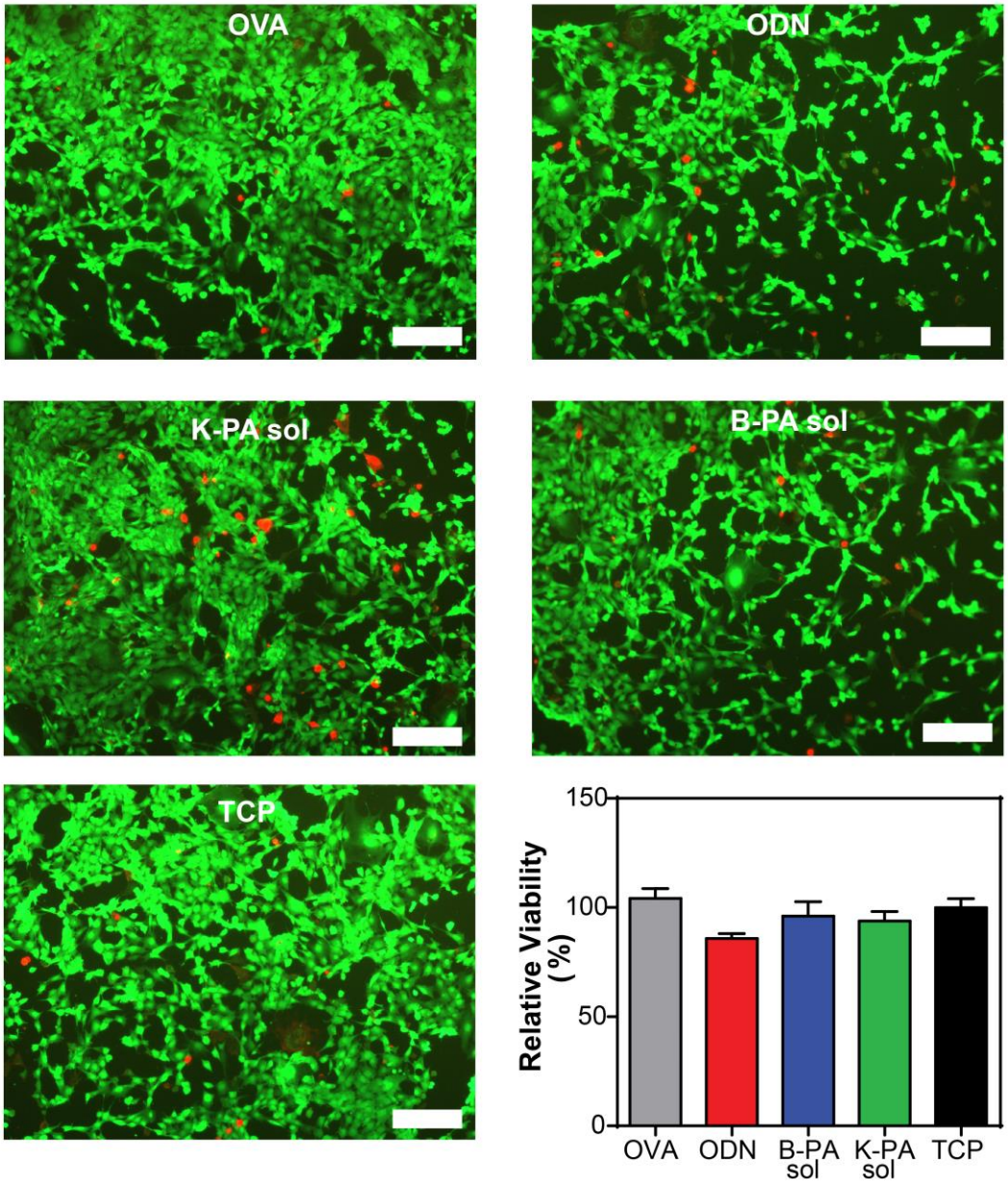

Figure 2.7 Cytotoxic effect of materials. Evaluation of cytotoxic effects of OVA, ODN and PA molecules on MEF cells with Live/Dead and Alamar Blue assays. (Statistical analysis was performed by using one-way ANOVA with Tukey's Multiple Comparison post-test. No significant difference was observed. Scale bar is 100 nm)

Cytotoxic results showed that the material was highly biocompatible with wild type mouse embryonic fibroblasts (wt MEF) (Figure 2.7).

2.3.2 Biotinylated ovalbumin binds to B-PA nanofibers

Ovalbumin (OVA) was chosen as the model antigen for the study of PA/ODN-mediated immune responses due to its widespread use in immunology research [88]. Streptavidin has four binding sites and an exceptionally high affinity for biotin, allowing the use of SA-biotin interactions for non-covalent antigen binding to the PA/ODN network [89]. Previous studies have demonstrated that OVA or OVA-derived sequences can be covalently bound to designed materials and raise directed immune responses [77, 90]. As such, we have bound biotinylated ovalbumin to self-assembling B-PA/ODN nanofibers through streptavidin-biotin linkages to produce a non-covalent equivalent to these systems.

To demonstrate that OVA is able to successfully bind to the peptide nanofibers, we visualized the nanostructure complex using immunogold staining. Transmission electron microscopy (TEM) was used to image the peptide nanofibers stained with gold nanoparticle conjugated antibodies against anti-ovalbumin (IgG-gold). IgG-gold (Figure 2.8 A) was observed to bind anti-ovalbumin in the B-PA/ODN complex (white dots in Figure 2.8 A), while no gold binding was observed when the primary antibody for ovalbumin was not used (Figure 2.8.B). These results show that biotinylated ovalbumin can bind to B-PA/ODN nanostructures through streptavidin-biotin

linkages. These results show that B-PA/ODN nanostructure is a promising carrier material for antigens.

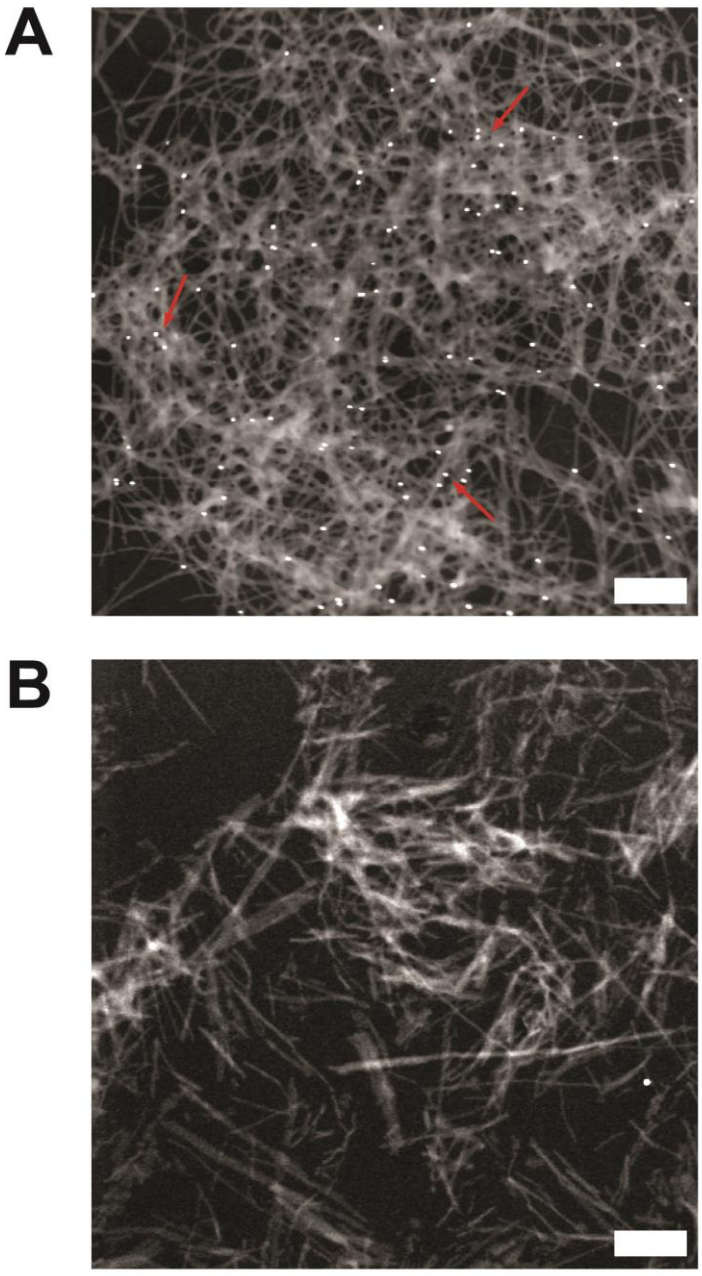

Figure 2.8 Antigen-bearing B-PA/ODN nanostructures. (A) STEM image of anti IgG-gold labeled B-PA/ODN + OVA nanostructures. Scale bar is 500 nm. (B) STEM image of anti IgG-gold labeled B-PA/ODN + OVA nanostructures without anti-Ovalbumin addition. Scale bar is 500 nm. (Shiny dots show gold nanoparticles)

2.3.3 Nanofiber size and epitope density can be controlled by dilution and non-OVA binding peptide incorporation

Peptide nanofibers are highly dynamic nanostructures and can be engineered to display an optimal set of properties for the development of controllable nanomaterials in biological applications [91, 92]. Nanomaterial size in particular is vital for determining the destination of any *in vivo* agent, and can be altered with relative freedom using PA structures. Nanomaterials measuring less than 50 nm in diameter target drying lymph nodes (dLNs) by passive diffusion/convection and are internalized by dendritic cells (DC) and macrophages residing in lymph nodes (LNs), but nanomaterials in the 500–2000 nm range are transported to dLNs by DC-mediated trafficking [93, 94]. The density and orientation of binding sites on the nanomaterial are also important to control the binding of antigens and optimize the presentation capacity of the structure [82].

As size control is a vital aspect of nanomaterial localization and clearance, TEM imaging was performed to investigate the effect of dilution on the sizes self-assembled B-PA/ODN nanostructures. Briefly, B-PA/ODN nanostructures were formed as mentioned in the materials and methods section. After the formation of nanostructures, self-assembled B-PA/ODN was diluted serially and STEM images were taken at each dilution. TEM images showed that the nanofibrous morphology of self-assembled nanostructures was not affected by serial dilution. However, after dilution, the density and sizes of nanostructures were reduced (Figure 2.9). These results suggest that it is possible to control the size of self-assembled nanomaterials by dilution.

Ovalbumin-PA nanostructure binding was further investigated to characterize the effect of dilution on the affinity between the components of the nanomaterial system (Figure 2.3.3.2.). Self-assembled B-PA/ODN nanostructures were formed, serially diluted and coated on ELISA plates. A standard ELISA protocol was then performed, and OVA was found to bind the B-PA/ODN nanostructures in a broad range of dilutions. These results are in agreement with our TEM images of diluted OVA/B-PA/ODN complexes (Figure 2.5 and Figure 2.10).

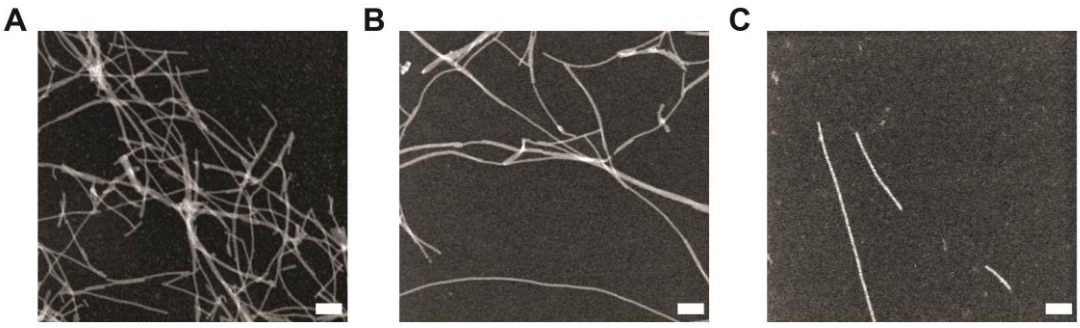

Figure 2.9 Morphological characterizations of diluted self-assembled B-PA/ODN nanostructures. A) STEM images of 0.023% (w/v) self-assembled B-PA/ODN nanostructure (stock). B) STEM images of 10-fold diluted self-assembled B-PA/ODN nanostructure. C) STEM images of 100-fold diluted self-assembled B-PA/ODN nanostructure. Scale bars are 100 nm.

In addition to concentration-dependent analyses, a non-OVA binding peptide amphiphile (K-PA) was also used as a spacer to demonstrate that the density of binding sites can be controlled within the nanostructure matrix. K-PA and B-PA were mixed at 1:1 molar ratio, left to form self-assembled nanostructures with ODN, and their binding capacity was investigated by ELISA. In contrast with other ELISA

experiments; the PA mixture and OVA were diluted in water rather than the assay buffer to minimize the effects of other ions. The optical density (OD) of the B-PA/K-PA mixture was reduced to about half of the B-PA/ODN nanostructure (Figure 2.10 B), suggesting that a non-OVA binding "spacer" can be used to reduce the number of binding sites without losing nanostructure formation (Figure 2.10). Such a mechanism can be utilized to optimize antigen presentation under conditions where distances between binding sites are important.

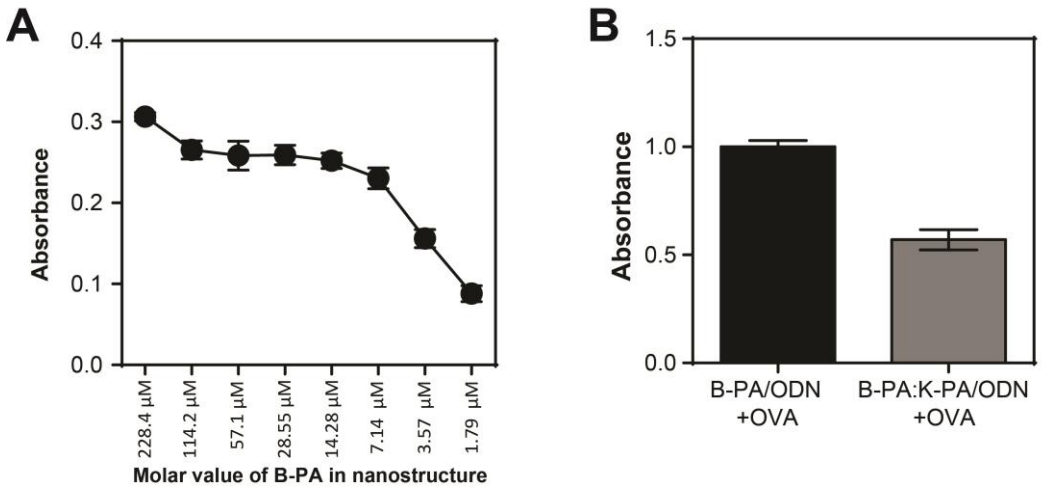

Figure 2.10 Control of antigen binding to PA/ODN nanostructure via ELISA. A) Demonstration of antigen ligation to B-PA/ODN nanostructure via dilution of self-assembled nanostructure. B) Demonstration of antigen ligation to B-PA/ODN or B-PA:K-PA/ODN nanostructure via changing antigen-binding site density. 228.4 µM of B-PA for B-PA/ODN+OVA and 114.2 µM of B-PA / K-PA (1:1) for B-PA:K-PA/ODN+OVA group were used for antigen-binding site density.

2.3.4 B-PA/ODN nanostructure complex promotes cytokine secretion

IFNγ and IL-12 are the cytokines responsible for directing the differentiation of the Th1 population during the primary antigen response, and serve to build a bridge between innate and adaptive immune responses by linking pathogen recognition through innate immune cells with the induction of antigen-specific immunity. IFNγ is also a critical mediator of anti-viral and anti-tumor responses, and plays a pivotal role in the immune detection and elimination of cancer cells [95-98]. IL-6, in contrast, directs the immune response towards a Th2 phenotype [99]. ODN1826 was previously shown to promote IL-12, IFNγ and IL-6 secretion from splenocytes and also modulate the immune response towards a Th1 phenotype [100]. To assess the immunomodulatory effect of the PA/ODN nanostructure, we treated splenocytes with PA/ODN and ODN *in vitro* at a final concentration of 1 μg/mL ODN1826. The amounts of cytokines in the culture supernatants were determined by ELISA. As shown in Figure 2.11, we found that the B-PA/ODN nanostructure dramatically promoted the expression of IFNγ, IL-12, and IL-6, while K-PA/ODN and ODN alone exhibited less pronounced immunostimulatory effects. However, in contrast to B-PA/ODN and ODN, K-PA/ODN was also observed to lower IL-6 secretion. This result is in agreement with our previous results [84] and suggests that the B-PA/ODN nanostructure elicits the secretion of IFNγ and IL-12 in splenocytes, and a similar effect was also proposed as the potential mechanism-of-action for ODN1826 [100].

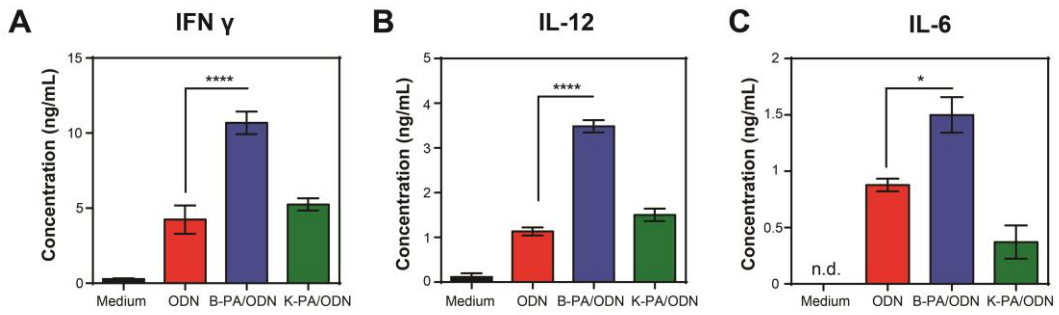

Figure 2.11 Cytokine secretion profile of splenocytes triggered by PA/ODN nanostructures and ODN. Mouse splenocytes were treated with the indicated formulations, and cytokine concentrations in culture media were detected with ELISA: A) IFNγ, B) IL-12, and C) IL-6. ODN concentration in all groups was 1 μg/mL. (*$p<0.05$, ****$p<0.001$ according to one-way ANOVA with Tukey's multiple comparison post-test) (n.d. indicates "not detected")

It is therefore possible for PA/ODN to alter the immune response toward a Th1 phenotype, and for the B-PA/ODN nanostructure in particular to enhance the cytokine-stimulating effect that ODN1826 exhibits on splenocytes. Since the therapeutic effects of IL-12 and IFNγ are well-characterized, these results also demonstrate that PA/ODN nanostructures can play a critical role in immunotherapeutic approaches that require the induction of cytokine secretion.

2.3.5 PA/ODN nanofibers enhance expression of the maturation markers and cross-presentation of antigens and uptake of ODN

Antigen presenting cells (APCs), including DCs, macrophages and B cells, are specialized cells that capture and engulf exogenous antigens through endocytosis, digest them to isolate the antigens they contain, and present these antigens to CD4+ or CD8+ T cells through MHC class II or class I molecules, respectively. In addition to stimulation by MHCs, the activation and proliferation of T-cells also requires the presence of co-stimulatory molecules such as CD80 and CD86. CD40 is expressed by APCs and serves as a co-simulator, while Toll like receptor agonists assist in this process by increasing the expression levels of co-stimulatory molecules [11, 101-105]. As ODN1826 functions as a TLR9 agonist, we have tested its ability to facilitate APC maturation in the presence and absence of a supporting peptide matrix [103]. To verify whether the PA/ODN nanostructure has the capability of promoting APC maturation, splenocytes were treated with (OVA+ODN), (B-PA/ODN+SA+OVA) and (K-PA/ODN+SA+OVA) for 24 h. These formulations were administered as proof-of-concept doses for future *in vivo* experiments and to observe the behavior of the material in clinical concentrations. As shown in Figure 2.12 A, B-PA/ODN and K-PA/ODN nanostructures significantly enhanced the expression of the APC-stimulating marker CD86 compared to the ODN+OVA mixture. B-PA/ODN and K-PA/ODN nanostructures also significantly enhanced the expression of CD40 compared to ODN+OVA (Figure 2.12. B). The K-PA/ODN nanostructure promoted both CD40 and CD86 expression to a greater extent than the B-PA/ODN nanostructure. These results

show that the B-PA/ODN nanostructure is able to effectively promote APC maturation through the upregulation of co-stimulatory molecules.

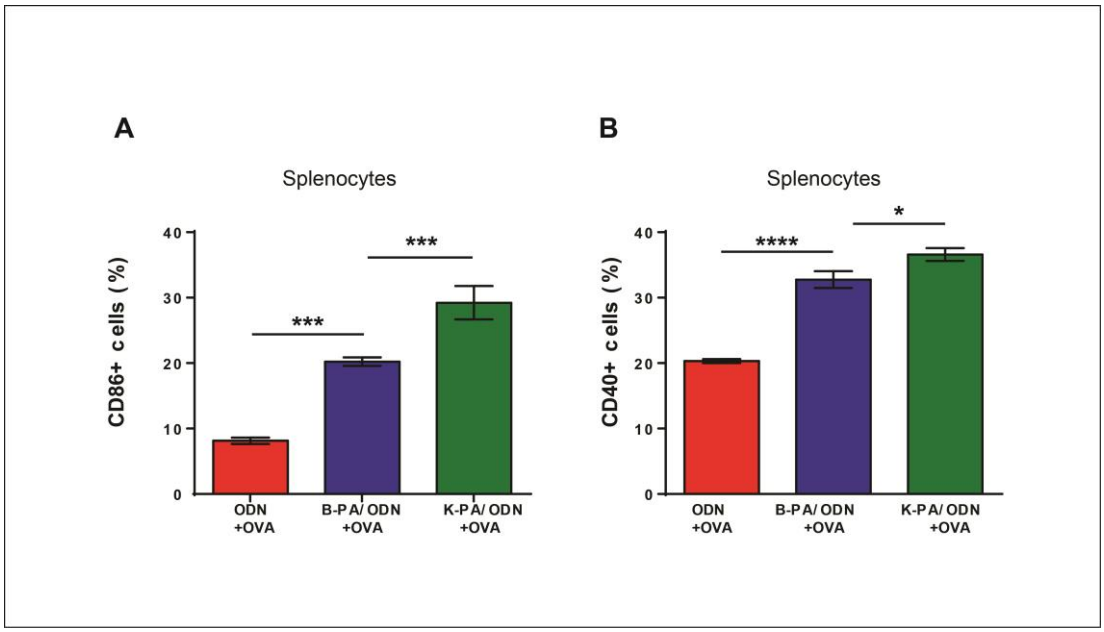

Figure 2.12 Effect of PA/ODN and OVA on maturation marker of splenocytes. A and B) flow-cytometry analysis of the expression of cell surface costimulatory markers CD40 and CD86 on splenocytes. (*$p<0.05$, ****$p<0.001$ according to one-way ANOVA with Tukey's multiple comparison post-test).

Cross-presentation involves the capture, endocytosis and presentation of extracellular antigens to naïve CD8+ T cells through MHC class I molecules [106, 107]. To verify whether PA/ODN nanostructures also exhibit the capability to promote the cross-presentation of OVA, splenocytes were treated with (B-PA/ODN+SA+OVA), (K-PA/ODN+SA+OVA) and (OVA+ODN) formulations. We have previously shown that

OVA binds to the B-PA/ODN nanostructure through an SA linker, but is incapable of binding to K-PA/ODN (due to the lack of biotin residues for SA linkers to connect on the K-PA/ODN nanostructure), allowing us to determine the importance of the linker and antigen-adjuvant proximity with regards to presentation efficiency (Figure 2.3.2.1). Cross-presentation of OVA was performed by flow cytometry. Cells were stained with a mAb that recognizes SIINFEKL complexed with H-2Kb.

As shown in Figure 2.13, the B-PA/ODN nanostructure promotes OVA presentation to a greater extent than the OVA+ODN formulation and K-PA/ODN nanostructure. As such, the presence of a functional SA-biotin bridge appears to be necessary for efficient cross-promotion by the peptide structure, and the non-covalent binding of an antigen to a PA matrix was much more successful in promoting cross-presentation compared to a mixture of non-bound antigens and PA networks. IFNγ is known to be important for cross-presentation and the promotion of MHC class I molecules [98], and our results agree with our previous suggestion that enhanced cytokine and IFNγ secretion by B-PA/ODN nanostructures could enhance the presentation of antigens (Figure 2.13.).

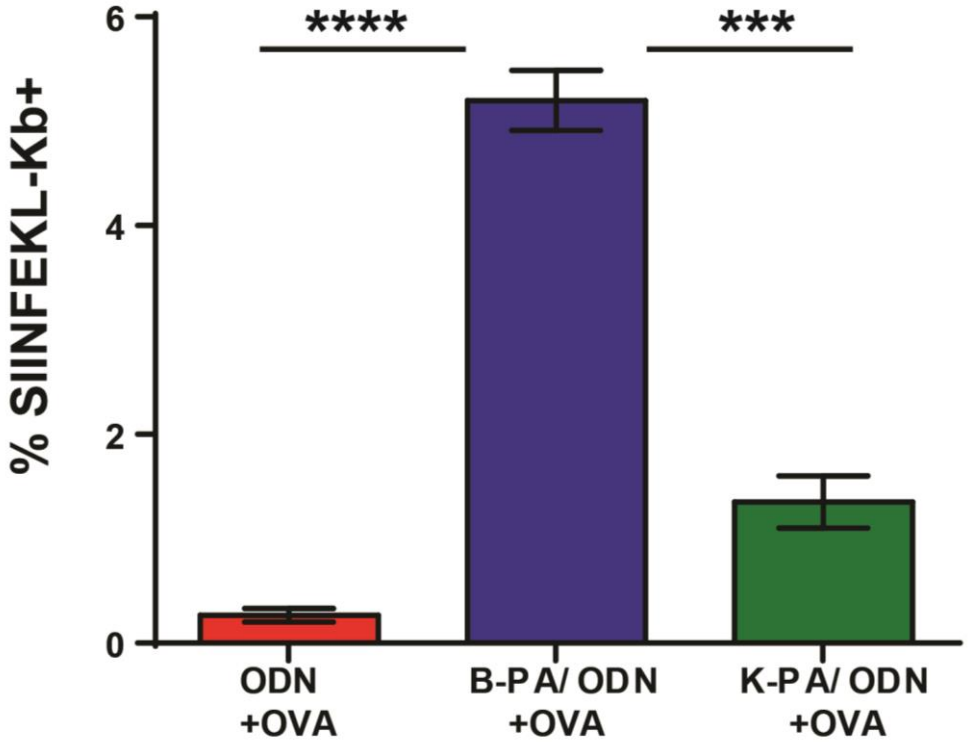

Figure 2.13 *In vitro* stimulation of immune responses by PA/ODN and OVA. Flow-cytometry analysis of cross-presentation of OVA on APC. (*p<0.05, ****p<0.001 according to one-way ANOVA with Tukey's multiple comparison post-test).

2.3.6 Effect of PA/ODN nanostructures on humoral immunity and splenocytes proliferation

The immunogenicity of some antigens is limited, and it is especially problematic to produce effective vaccines incorporating these antigens [57]. As such, the potency of the B-PA/ODN nanostructure as a vaccine system was studied *in vivo* to determine its ability to increase the immunogenicity of a model antigen. To understand the effect of the B-PA/ODN nanostructure on the immunogenicity of OVA, mice were immunized subcutaneously with different formulations of vaccines twice at day 0 and day 15. The treatment groups were B-PA/ODN+OVA (with SA as a linker), and K-PA/ODN (with SA present within the mixture) and OVA+ODN used as positive control [46]. The antibody titer against antigen is an important indicator for the evaluation of humoral immune responses [11]. Consequently, blood was collected from animals at day 21 and OVA-specific IgG levels in sera were analyzed to determine this value for each group. The OVA+ODN and K-PA/ODN+OVA formulations were found to exhibit milder immune responses than the B-PA/ODN+OVA nanostructure formation, while B-PA/ODN+OVA could induce a significantly higher anti-OVA IgG antibody production (Figure 2.14). The K-PA/ODN+OVA nanostructure formulation induced a comparable immune response to the ODN+OVA formulation, with no significant difference between the two. These results indicate that the B-PA/ODN nanostructure could strongly enhance the immune response *in vivo*, and that the observed effect was attributable to the close association between the antigen and the PA/ODN complex. It

can thus be concluded that the B-PA/ODN nanostructure is able to effectively promote the specific adaptive immune response against the co-delivered antigen.

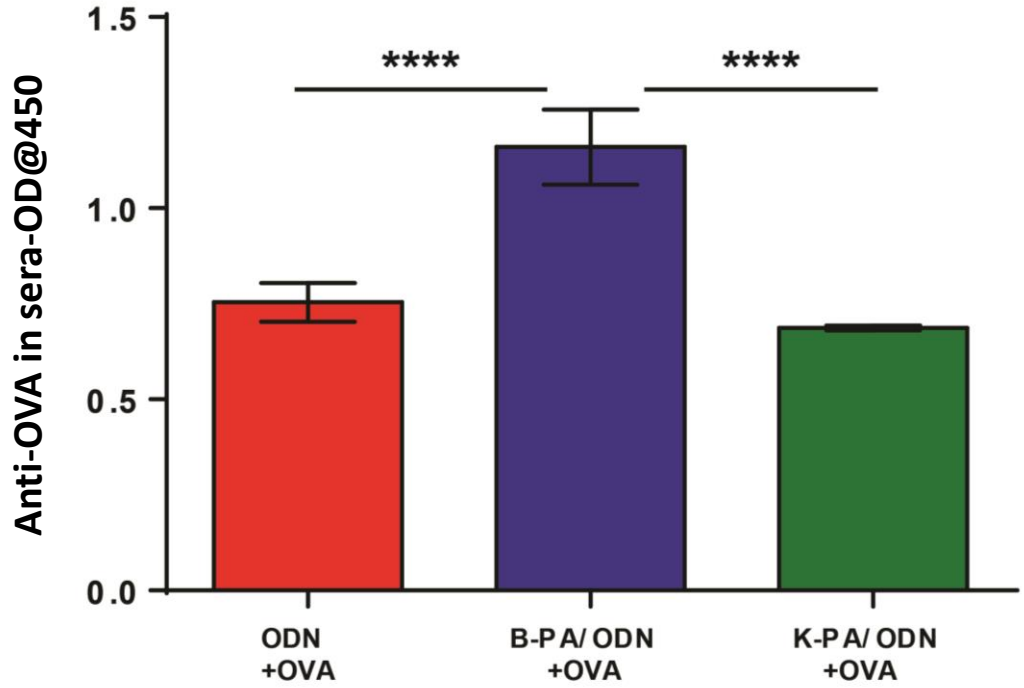

Figure 2.14 *In vivo* immunization with PA/ODN versus soluble antigen or antigen with ODN. OVA-specific antibody production in sera from mice immunized with different groups. Seven days after second injection, sera were isolated from mice and analyzed for IgG levels by ELISA (using 10-fold diluted sera). (*$p<0.05$, ****$p<0.0001$ according to one-way and two-way ANOVA with Tukey's multiple comparison post-test). Bars shown are mean ± SEM (n = 5)

The effect of PA/ODN complexes on the relative frequency of IgG isotopes was also tested, and the ODN+OVA and K-PA/ODN formulations were found to enhance the

production of IgG to a greater extent than the B-PA/ODN nanostructure (Figure 2.15). Interestingly, B-PA/ODN nanostructure significantly enhanced IgG2a production compared to other formulations (Figure 2.15). There was no significant difference between OVA+ODN and K-PA/ODN in the induction of IgG1 and IgG2a antibody responses. It is well-recognized that IgG1 and IgG2 isotopes are boosted by Th2 cytokines (such as IL-4 and IL-6) and Th1 cytokines (such as IFN-γ), respectively. Therefore, it can be concluded that B-PA/ODN nanostructure is able to direct the humoral response towards the Th1 pathways. Cytokine profiles of B-PA/ODN nanostructures are also support this conclusion (Figure 2.11).

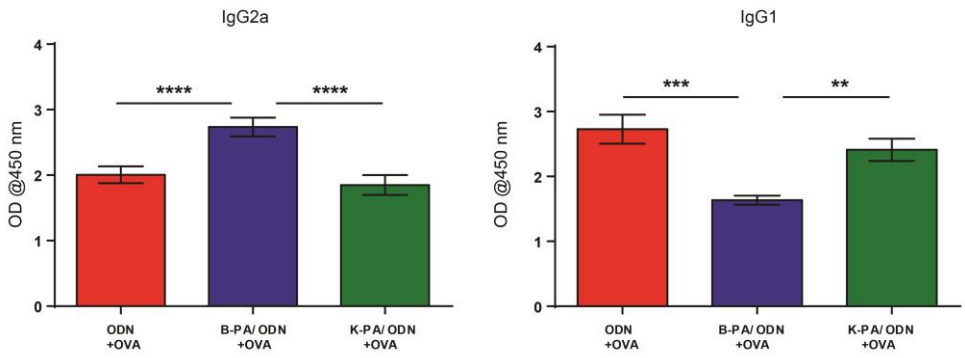

Figure 2.15 IgG isotopes in sera of immunized mice with PA/ODN versus soluble antigen or antigen with ODN. OVA-specific antibody production in sera from mice immunized with different groups. Seven days after second injection, sera were isolated from mice and analyzed for IgG2a and IgG1 levels by ELISA (using 10-fold diluted sera). (*$p<0.05$, ****$p<0.0001$ according to one-way and two-way ANOVA with Tukey's multiple comparison post-test). Bars shown are mean ± SEM (n = 5)

T cell activation is important for vaccine performance, and CD8+ T cells are especially crucial for conditions such as intracellular infections and cancer. To promote the differentiation of functional T cells, the vaccine material should facilitate antigen entry into MHC class I or II processing pathways, trigger dendritic cell (DC) activation, and induce interferon (IFN) production [46, 49, 108, 109]. To assess the effect of PA/ODN nanostructures on the proliferation of splenocytes (including T cells), spleens from immunized mice (one week after second injection) were removed and the splenocytes were isolated. These splenocytes were restimulated with OVA and a standard BrdU assay was performed. As shown in Figure 2.16, the B-PA/ODN nanostructure significantly promoted splenocyte proliferation compared to other groups when the splenocytes were restimulated with OVA. Moreover, no proliferation was observed in any of the groups when splenocytes were treated with cell medium. These results show that the B-PA/ODN nanostructure could significantly promote antigen-specific splenocyte proliferation, and agree with prior results obtained from SIINFEKL presentations (Figure 2.13.). Thus, we further support our previous conclusions that the B-PA/ODN nanostructure promotes antigen presentation and raises specific adaptive immune response against the co-delivered antigen.

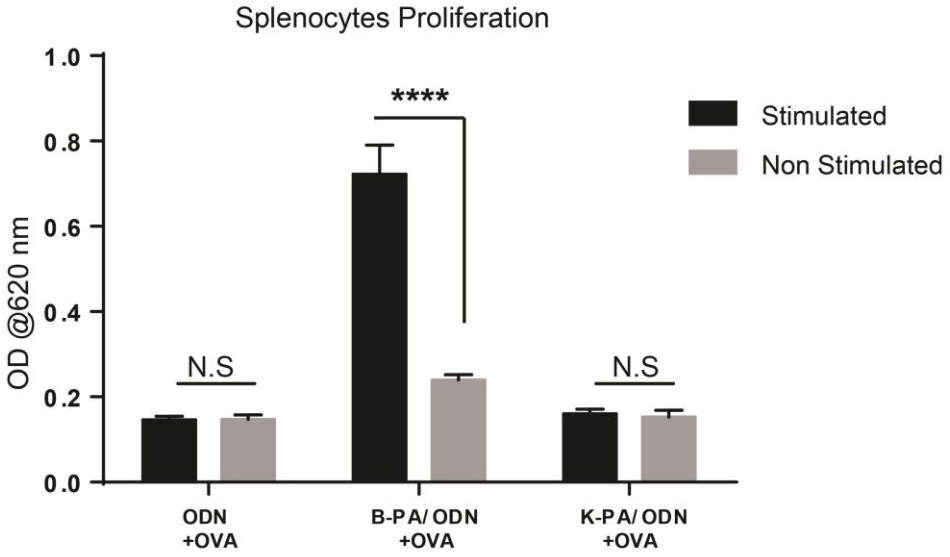

Figure 2.16 Splenocytes proliferation of immunized mice with PA/ODN versus soluble antigen or antigen with ODN. The effect of PA/ODN, OVA and OVA+ODN on splenocyte proliferation. Splenocyte proliferation was measured by BrdU assay after *ex vivo* restimulation of splenocytes with OVA *in vitro*. (*$p<0.05$, ****$p<0.0001$ according to one-way and two-way ANOVA with Tukey's multiple comparison post-test). Bars shown are mean ± SEM (n = 5)

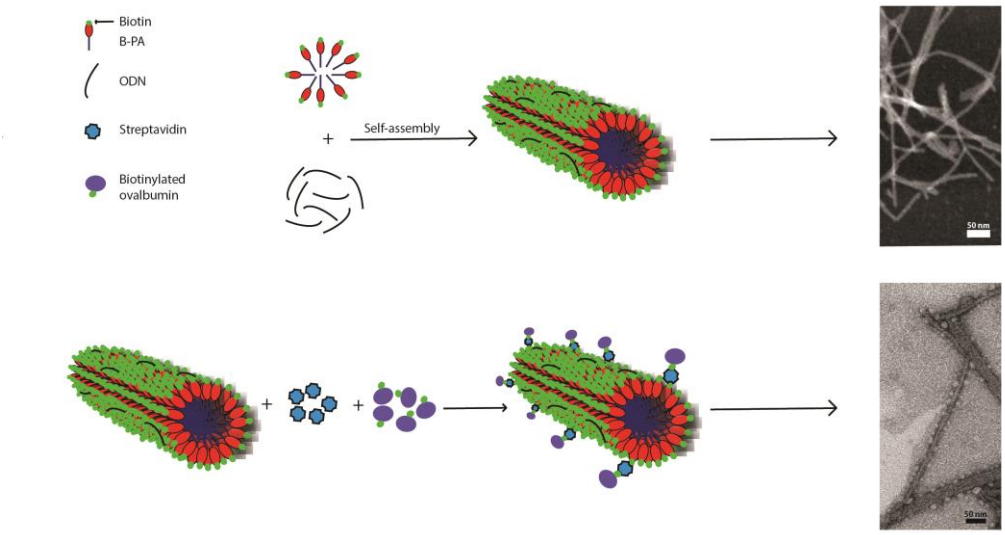

Figure 2.17 Schematic illustration of B-PA nanofiber formation and associated transmission electron microscope images.

Finally, effect of PAs on ODN uptake was demonstrated. As shown in Figure 2.18, B-PA/ODN nanostructure was uptake more than K-PA/ODN and only ODN formulation. As a result, B-PA/ODN nanostructure enhances uptake mechanism of ODN, and ovalbumin bound B-PA/ODN nanostructure promote antigens uptake as well. This result is consistent with the previous result of SIINFELK presentation (Figure 2.13).

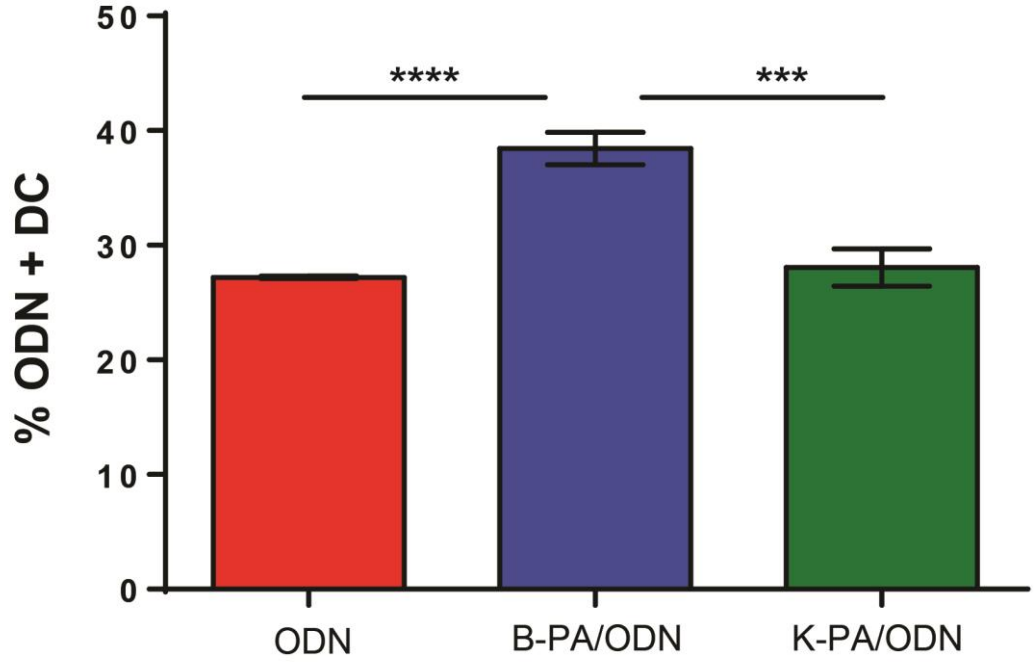

Figure 2.18 Effect of PAs on the cellular uptake of FITC-ODN in dendritic cells. Flow-cytometry analysis of the uptake of FITC labeled ODN on dendritic cells of spleen. (*p<0.05, ****p<0.001 according to one-way ANOVA with Tukey's multiple comparison post-test).

CHAPTER 3

3. Conclusions and future perspectives

PAs can self-assemble into a range of novel nanostructures, which is what makes them so attractive to be used for different purposes. Due to the properties of tailorable bioactive epitopes, a lot of studies have been done for understanding the effects of PAs on biological systems. Moreover, self-assembled peptides are attractive because of their ease of design, biocompatibility, defined functional motifs, fast response to external environment, biodegradability, and low immunogenicity as well as bioactivity. Rationally designed biomaterials allow us to solve a wide range of health problems. Infectious diseases, autoimmune immune diseases, neurodegenerative diseases, organ failures, and wound healing can be treated with rationally designed biomaterials. Recent developments in materials science and biology have greatly broadened the scope of intelligent biomaterial design for therapeutic applications, as these materials can now be synthesized, functionalized, characterized, controlled and mass produced with considerable ease. In this thesis, self-assembled biotinylated peptide amphiphile nanofibers were utilized for tuning the immune response against a specific antigen that is noncovalently attached to the peptide nanofibers.

In this study, we report the first example of a cylindrical nanostructure complex that is formed through the self-assembly of peptide amphiphile and ODN components and acts as an efficient vaccine nanocarrier for modulating the humoral and cellular immune responses in mice. Firstly, B-PA and K-PA peptide amphiphile molecules were designed and synthesized with solid phase peptide synthesis. All PA molecules

were purified with High Performance Liquid Chromatography (HPLC), and their purity and mass spectra peaks were analyzed by using Liquid Chromatography and Mass Spectrometry (LC-MS). Our results indicated that both PAs were highly pure and their masses were consistent with expected ones. We demonstrated that biotinylated peptide amphiphiles (B-PAs), co-assembled in conjunction with ODNs form cylindrical nanostructures that incorporate biotin linker structures for antigen attachment. Antigens possessing SA-linker regions were shown to attach readily onto this structure, and the non-biotinylated K-PA could be utilized to alter the overall epitope density on the structure. This novel configuration allows the rapid, non-covalent attachment of a broad variety of antigen types to a universal "presentation matrix" composed of PA and ODN components.

We also demonstrated that the size of self-assembled PA/ODN nanostructures could be altered through dilution. In addition, the B-PA/ODN cylindrical nanostructure strongly induced antibody production and secretion of stimulatory cytokines, thereby directing the immune response towards the Th1 type. Further investigations have revealed that immune induction by B-PA/ODN nanostructures depends heavily on their ability to enhance antigen uptake, induce dendritic cell maturation and promote cross-presentation. Many of these properties are not present when the antigen is co-delivered (but not covalently attached) to the PA/ODN matrix, suggesting that the close proximity between the antigen and the adjuvant material plays an important role in antigen presentation.

Overall, our PA/ODN nanostructure enables the presentation of viral, bacterial or tumor antigenic peptides on a single platform, enhances the immunogenicity of attached proteins, and promotes their cross-presentation, addressing many of the shortcomings associated with modern vaccine development [110]. We therefore suggest that these materials can be efficiently used for vaccine delivery in the treatment of a broad variety of disorders, and that they would be especially suitable for combating newly emerging diseases that necessitate the rapid development of vaccines.

Bibliography

[1] G. M. Whitesides and B. Grzybowski, "Self-assembly at all scales," *Science,* vol. 295, pp. 2418-2421, 2002.

[2] D. Philp and J. F. Stoddart, "Self - assembly in natural and unnatural systems," *Angewandte Chemie International Edition in English,* vol. 35, pp. 1154-1196, 1996.

[3] A. Dehsorkhi, V. Castelletto, and I. W. Hamley, "Self - assembling amphiphilic peptides," *Journal of Peptide Science,* vol. 20, pp. 453-467, 2014.

[4] H. Cui, M. J. Webber, and S. I. Stupp, "Self - assembly of peptide amphiphiles: From molecules to nanostructures to biomaterials," *Peptide Science,* vol. 94, pp. 1-18, 2010.

[5] J. D. Hartgerink, E. Beniash, and S. I. Stupp, "Peptide-amphiphile nanofibers: a versatile scaffold for the preparation of self-assembling materials," *Proceedings of the National Academy of Sciences,* vol. 99, pp. 5133-5138, 2002.

[6] M. O. Guler, L. Hsu, S. Soukasene, D. A. Harrington, J. F. Hulvat, and S. I. Stupp, "Presentation of RGDS epitopes on self-assembled nanofibers of branched peptide amphiphiles," *Biomacromolecules,* vol. 7, pp. 1855-1863, 2006.

[7] S. E. Paramonov, H.-W. Jun, and J. D. Hartgerink, "Self-assembly of peptide-amphiphile nanofibers: the roles of hydrogen bonding and amphiphilic packing," *Journal of the American Chemical Society,* vol. 128, pp. 7291-7298, 2006.

[8] E. De Santis and M. G. Ryadnov, "Peptide self-assembly for nanomaterials: the old new kid on the block," *Chemical Society Reviews,* vol. 44, pp. 8288-8300, 2015.

[9] G. A. Hudalla, T. Sun, J. Z. Gasiorowski, H. Han, Y. F. Tian, A. S. Chong, *et al.*, "Gradated assembly of multiple proteins into supramolecular nanomaterials," *Nature materials,* vol. 13, p. 829, 2014.

[10] C. A. Hauser and S. Zhang, "Designer self-assembling peptide nanofiber biological materials," *Chemical Society Reviews,* vol. 39, pp. 2780-2790, 2010.

[11] H. Wang, Z. Luo, Y. Wang, T. He, C. Yang, C. Ren, *et al.*, "Enzyme - Catalyzed Formation of Supramolecular Hydrogels as Promising Vaccine Adjuvants," *Advanced Functional Materials,* 2016.

[12] B. Mammadov, R. Mammadov, M. O. Guler, and A. B. Tekinay, "Cooperative effect of heparan sulfate and laminin mimetic peptide nanofibers on the promotion of neurite outgrowth," *Acta biomaterialia,* vol. 8, pp. 2077-2086, 2012.

[13] G. A. Silva, C. Czeisler, K. L. Niece, E. Beniash, D. A. Harrington, J. A. Kessler, *et al.*, "Selective differentiation of neural progenitor cells by high-epitope density nanofibers," *Science,* vol. 303, pp. 1352-1355, 2004.

[14] A. Tan, J. Rajadas, and A. M. Seifalian, "Biochemical engineering nerve conduits using peptide amphiphiles," *Journal of controlled release,* vol. 163, pp. 342-352, 2012.

[15] S. Khan, S. Sur, P. Y. Dankers, R. M. da Silva, J. Boekhoven, T. A. Poor, *et al.*, "Post-assembly functionalization of supramolecular nanostructures with bioactive peptides and fluorescent proteins by native chemical ligation," *Bioconjugate chemistry*, vol. 25, pp. 707-717, 2014.
[16] Z. D. Mumcuoğlu, "Self-assembled peptide nanostructure delivery sytems for oligonucleotide therapy," Bilkent University.
[17] D. Mumcuoglu, M. Sardan, T. Tekinay, M. O. Guler, and A. B. Tekinay, "Oligonucleotide Delivery with Cell Surface Binding and Cell Penetrating Peptide Amphiphile Nanospheres," *Molecular pharmaceutics*, vol. 12, pp. 1584-1591, 2015.
[18] R. Mammadov, G. Cinar, N. Gunduz, M. Goktas, H. Kayhan, S. Tohumeken, *et al.*, "Virus-like nanostructures for tuning immune response," *Scientific reports*, vol. 5, 2015.
[19] C. E. McMurran, C. A. Jones, D. C. Fitzgerald, and R. J. Franklin, "CNS remyelination and the innate immune system," *Frontiers in Cell and Developmental Biology*, vol. 4, 2016.
[20] B. Alberts, A. Johnson, J. Lewis, M. Raff, K. Roberts, and P. Walter, "Innate immunity," 2002.
[21] G. Mayer, "Immunology-Chapter Two: Complement," *Microbiology and Immunology On-Line Textbook*, 2006.
[22] G. S. Hotamisligil, "Inflammation and metabolic disorders," *Nature*, vol. 444, pp. 860-867, 2006.
[23] L. M. Coussens and Z. Werb, "Inflammation and cancer," *Nature*, vol. 420, pp. 860-867, 2002.
[24] C. Janeway, K. P. Murphy, P. Travers, and M. Walport, *Janeway's immunobiology*: Garland Science, 2008.
[25] L. D. Wang and A. J. Wagers, "Dynamic niches in the origination and differentiation of haematopoietic stem cells," *Nature reviews Molecular cell biology*, vol. 12, pp. 643-655, 2011.
[26] C. A. Biron, K. B. Nguyen, G. C. Pien, L. P. Cousens, and T. P. Salazar-Mather, "Natural killer cells in antiviral defense: function and regulation by innate cytokines," *Annual review of immunology*, vol. 17, pp. 189-220, 1999.
[27] W. M. Yokoyama, "Natural killer cell immune responses," *Immunologic research*, vol. 32, pp. 317-325, 2005.
[28] J. C. Sun and L. L. Lanier, "Natural killer cells remember: an evolutionary bridge between innate and adaptive immunity?," *European journal of immunology*, vol. 39, pp. 2059-2064, 2009.
[29] J. Banchereau and R. M. Steinman, "Dendritic cells and the control of immunity," *Nature*, vol. 392, pp. 245-252, 1998.
[30] J. Banchereau, F. Briere, C. Caux, J. Davoust, S. Lebecque, Y.-J. Liu, *et al.*, "Immunobiology of dendritic cells," *Annual review of immunology*, vol. 18, pp. 767-811, 2000.
[31] R. M. Steinman and H. Hemmi, "Dendritic cells: translating innate to adaptive immunity," in *From Innate Immunity to Immunological Memory*, ed: Springer, 2006, pp. 17-58.

[32] M. J. Spiering, "Primer on the Immune System," *Alcohol research: current reviews,* vol. 37, p. 171, 2015.
[33] J. Leor, D. Palevski, U. Amit, and T. Konfino, "Macrophages and regeneration: Lessons from the heart," in *Seminars in cell & developmental biology*, 2016.
[34] J. L. Stow and N. D. Condon, "The cell surface environment for pathogen recognition and entry," *Clinical & Translational Immunology,* vol. 5, p. e71, 2016.
[35] K. Hoebe, X. Du, P. Georgel, E. Janssen, K. Tabeta, S. Kim, *et al.*, "Identification of Lps2 as a key transducer of MyD88-independent TIR signalling," *Nature*, vol. 424, pp. 743-748, 2003.
[36] S. Akira, S. Uematsu, and O. Takeuchi, "Pathogen recognition and innate immunity," *Cell,* vol. 124, pp. 783-801, 2006.
[37] H. S. Warren, "Toll-like receptors," *Critical care medicine,* vol. 33, pp. S457-S459, 2005.
[38] B. Lemaitre, E. Nicolas, L. Michaut, J.-M. Reichhart, and J. A. Hoffmann, "The dorsoventral regulatory gene cassette spätzle/Toll/cactus controls the potent antifungal response in Drosophila adults," *Cell,* vol. 86, pp. 973-983, 1996.
[39] J. M. Blander and R. Medzhitov, "Regulation of phagosome maturation by signals from toll-like receptors," *Science,* vol. 304, pp. 1014-1018, 2004.
[40] A. Aderem and R. J. Ulevitch, "Toll-like receptors in the induction of the innate immune response," *Nature,* vol. 406, pp. 782-787, 2000.
[41] A. M. Krieg, "CPG motifs in bacterial dna and their immune effects*," *Annual review of immunology,* vol. 20, pp. 709-760, 2002.
[42] P. Ahmad - Nejad, H. Häcker, M. Rutz, S. Bauer, R. M. Vabulas, and H. Wagner, "Bacterial CpG - DNA and lipopolysaccharides activate Toll - like receptors at distinct cellular compartments," *European journal of immunology,* vol. 32, pp. 1958-1968, 2002.
[43] S. H. Kaufmann, "The contribution of immunology to the rational design of novel antibacterial vaccines," *Nature Reviews Microbiology,* vol. 5, pp. 491-504, 2007.
[44] N. A. Gow, F. L. van de Veerdonk, A. J. Brown, and M. G. Netea, "Candida albicans morphogenesis and host defence: discriminating invasion from colonization," *Nature Reviews Microbiology,* vol. 10, pp. 112-122, 2012.
[45] F. Steinhagen, T. Kinjo, C. Bode, and D. M. Klinman, "TLR-based immune adjuvants," *Vaccine,* vol. 29, pp. 3341-3355, 2011.
[46] R. L. Coffman, A. Sher, and R. A. Seder, "Vaccine adjuvants: putting innate immunity to work," *Immunity,* vol. 33, pp. 492-503, 2010.
[47] G. Douce, C. Turcotte, I. Cropley, M. Roberts, M. Pizza, M. Domenghini, *et al.*, "Mutants of Escherichia coli heat-labile toxin lacking ADP-ribosyltransferase activity act as nontoxic, mucosal adjuvants," *Proceedings of the National Academy of Sciences,* vol. 92, pp. 1644-1648, 1995.
[48] M. J. McElrath, "Selection of potent immunological adjuvants for vaccine construction," in *Seminars in cancer biology*, 1995, pp. 375-385.
[49] R. Edelman, "The development and use of vaccine adjuvants," *Molecular biotechnology,* vol. 21, pp. 129-148, 2002.

[50] S. Awate, L. A. Babiuk, and G. Mutwiri, "Mechanisms of action of adjuvants," *Front Immunol,* vol. 4, pp. 1-10, 2013.
[51] G. J. Nabel, "Designing tomorrow's vaccines," *New England Journal of Medicine,* vol. 368, pp. 551-560, 2013.
[52] D. Wu, Y. Gao, Y. Qi, L. Chen, Y. Ma, and Y. Li, "Peptide-based cancer therapy: opportunity and challenge," *Cancer letters,* vol. 351, pp. 13-22, 2014.
[53] E. I. Bah, M.-C. Lamah, T. Fletcher, S. T. Jacob, D. M. Brett-Major, A. A. Sall, *et al.*, "Clinical presentation of patients with Ebola virus disease in Conakry, Guinea," *New England Journal of Medicine,* vol. 372, pp. 40-47, 2015.
[54] L. R. Petersen, D. J. Jamieson, A. M. Powers, and M. A. Honein, "Zika virus," *New England Journal of Medicine,* vol. 374, pp. 1552-1563, 2016.
[55] J. Conniot, J. M. Silva, J. G. Fernandes, L. C. Silva, R. Gaspar, S. Brocchini, *et al.*, "Cancer immunotherapy: nanodelivery approaches for immune cell targeting and tracking," *Frontiers in chemistry,* vol. 2, p. 105, 2014.
[56] C. D. Mathers and D. Loncar, "Projections of global mortality and burden of disease from 2002 to 2030," *Plos med,* vol. 3, p. e442, 2006.
[57] N. Petrovsky and J. C. Aguilar, "Vaccine adjuvants: current state and future trends," *Immunology and cell biology,* vol. 82, pp. 488-496, 2004.
[58] B. D. Walker and D. R. Burton, "Toward an AIDS vaccine," *science,* vol. 320, pp. 760-764, 2008.
[59] S. G. Reed, S. Bertholet, R. N. Coler, and M. Friede, "New horizons in adjuvants for vaccine development," *Trends in immunology,* vol. 30, pp. 23-32, 2009.
[60] N. Zhang, R. Channappanavar, C. Ma, L. Wang, J. Tang, T. Garron, *et al.*, "Identification of an ideal adjuvant for receptor-binding domain-based subunit vaccines against Middle East respiratory syndrome coronavirus," *Cellular & molecular immunology,* 2015.
[61] A. Bråve, K. Ljungberg, B. Wahren, and M. A. Liu, "Vaccine delivery methods using viral vectors," *Molecular pharmaceutics,* vol. 4, pp. 18-32, 2007.
[62] C. Foged, "Subunit vaccines of the future: the need for safe, customized and optimized particulate delivery systems," *Therapeutic delivery,* vol. 2, pp. 1057-1077, 2011.
[63] J. J. Moon, H. Suh, A. Bershteyn, M. T. Stephan, H. Liu, B. Huang, *et al.*, "Interbilayer-crosslinked multilamellar vesicles as synthetic vaccines for potent humoral and cellular immune responses," *Nature materials,* vol. 10, pp. 243-251, 2011.
[64] E. Fragapane, R. Gasparini, F. Schioppa, F. Laghi-Pasini, E. Montomoli, and A. Banzhoff, "A heterologous MF59-adjuvanted H5N1 prepandemic influenza booster vaccine induces a robust, cross-reactive immune response in adults and the elderly," *Clinical and Vaccine Immunology,* vol. 17, pp. 1817-1819, 2010.
[65] I. D. Davis, W. Chen, H. Jackson, P. Parente, M. Shackleton, W. Hopkins, *et al.*, "Recombinant NY-ESO-1 protein with ISCOMATRIX adjuvant induces broad integrated antibody and CD4+ and CD8+ T cell responses in humans," *Proceedings of the National Academy of Sciences of the United States of America,* vol. 101, pp. 10697-10702, 2004.

[66] L. E. Guimarães, B. Baker, C. Perricone, and Y. Shoenfeld, "Vaccines, adjuvants and autoimmunity," *Pharmacological research,* vol. 100, pp. 190-209, 2015.
[67] P. Traquina, M. Morandi, M. Contorni, and G. Van Nest, "MF59 adjuvant enhances the antibody response to recombinant hepatitis B surface antigen vaccine in primates," *Journal of Infectious Diseases,* vol. 174, pp. 1168-1175, 1996.
[68] E. Schlosser, M. Mueller, S. Fischer, S. Basta, D. H. Busch, B. Gander, *et al.*, "TLR ligands and antigen need to be coencapsulated into the same biodegradable microsphere for the generation of potent cytotoxic T lymphocyte responses," *Vaccine,* vol. 26, pp. 1626-1637, 2008.
[69] P. Couvreur and C. Vauthier, "Nanotechnology: intelligent design to treat complex disease," *Pharmaceutical research,* vol. 23, pp. 1417-1450, 2006.
[70] T. Uto, T. Akagi, M. Toyama, Y. Nishi, F. Shima, M. Akashi, *et al.*, "Comparative activity of biodegradable nanoparticles with aluminum adjuvants: antigen uptake by dendritic cells and induction of immune response in mice," *Immunology letters,* vol. 140, pp. 36-43, 2011.
[71] J. S. Rudra, Y. F. Tian, J. P. Jung, and J. H. Collier, "A self-assembling peptide acting as an immune adjuvant," *Proceedings of the National Academy of Sciences,* vol. 107, pp. 622-627, 2010.
[72] B. Gungor, F. C. Yagci, G. Tincer, B. Bayyurt, E. Alpdundar, S. Yildiz, *et al.*, "CpG ODN nanorings induce IFNα from plasmacytoid dendritic cells and demonstrate potent vaccine adjuvant activity," *Science translational medicine,* vol. 6, pp. 235ra61-235ra61, 2014.
[73] M. F. Bachmann and G. T. Jennings, "Vaccine delivery: a matter of size, geometry, kinetics and molecular patterns," *Nature Reviews Immunology,* vol. 10, pp. 787-796, 2010.
[74] A. Gregory, R. Titball, and D. Williamson, "Vaccine delivery using nanoparticles. Front Cell Infect Microbiol 2013; 3: 13; PMID: 23532930," ed, 2013.
[75] V. B. Joshi, S. M. Geary, and A. K. Salem, "Biodegradable particles as vaccine delivery systems: size matters," *The AAPS journal,* vol. 15, pp. 85-94, 2013.
[76] A. Jegerlehner, T. Storni, G. Lipowsky, M. Schmid, P. Pumpens, and M. F. Bachmann, "Regulation of IgG antibody responses by epitope density and CD21 - mediated costimulation," *European journal of immunology,* vol. 32, pp. 3305-3314, 2002.
[77] M. Black, A. Trent, Y. Kostenko, J. S. Lee, C. Olive, and M. Tirrell, "Self - Assembled Peptide Amphiphile Micelles Containing a Cytotoxic T - Cell Epitope Promote a Protective Immune Response In Vivo," *Advanced Materials,* vol. 24, pp. 3845-3849, 2012.
[78] J. S. Rudra, T. Sun, K. C. Bird, M. D. Daniels, J. Z. Gasiorowski, A. S. Chong, *et al.*, "Modulating adaptive immune responses to peptide self-assemblies," *Acs Nano,* vol. 6, pp. 1557-1564, 2012.
[79] G. A. Hudalla, J. A. Modica, Y. F. Tian, J. S. Rudra, A. S. Chong, T. Sun, *et al.*, "A Self - Adjuvanting Supramolecular Vaccine Carrying a Folded Protein Antigen," *Advanced healthcare materials,* vol. 2, pp. 1114-1119, 2013.

[80] A. Trent, B. D. Ulery, M. J. Black, J. C. Barrett, S. Liang, Y. Kostenko, *et al.*, "Peptide amphiphile micelles self-adjuvant group A streptococcal vaccination," *The AAPS journal*, vol. 17, pp. 380-388, 2015.

[81] A. Holmberg, A. Blomstergren, O. Nord, M. Lukacs, J. Lundeberg, and M. Uhlen, "The biotin - streptavidin interaction can be reversibly broken using water at elevated temperatures," *Electrophoresis*, vol. 26, pp. 501-510, 2005.

[82] M. E. Davis, P. C. Hsieh, T. Takahashi, Q. Song, S. Zhang, R. D. Kamm, *et al.*, "Local myocardial insulin-like growth factor 1 (IGF-1) delivery with biotinylated peptide nanofibers improves cell therapy for myocardial infarction," *Proceedings of the National Academy of Sciences*, vol. 103, pp. 8155-8160, 2006.

[83] J. Pohar, D. Lainšček, R. Fukui, C. Yamamoto, K. Miyake, R. Jerala, *et al.*, "Species-specific minimal sequence motif for oligodeoxyribonucleotides activating mouse TLR9," *The Journal of Immunology*, vol. 195, pp. 4396-4405, 2015.

[84] R. Mammadov, G. Cinar, N. Gunduz, M. Goktas, H. Kayhan, S. Tohumeken, *et al.*, "Virus-like nanostructures for tuning immune response," *Sci Rep*, vol. 5, p. 16728, 2015.

[85] R. Mammadov, B. Mammadov, M. O. Guler, and A. B. Tekinay, "Growth factor binding on heparin mimetic peptide nanofibers," *Biomacromolecules*, vol. 13, pp. 3311-3319, 2012.

[86] H. Cui, M. J. Webber, and S. I. Stupp, "Self-assembly of peptide amphiphiles: from molecules to nanostructures to biomaterials," *Biopolymers*, vol. 94, pp. 1-18, 2010.

[87] D. Mumcuoglu, M. Sardan Ekiz, G. Gunay, T. Tekinay, A. B. Tekinay, and M. O. Guler, "Cellular Internalization of Therapeutic Oligonucleotides by Peptide Amphiphile Nanofibers and Nanospheres," *ACS Appl Mater Interfaces*, vol. 8, pp. 11280-7, May 11 2016.

[88] H.-X. Sun, Y.-P. Ye, H.-J. Pan, and Y.-J. Pan, "Adjuvant effect of Panax notoginseng saponins on the immune responses to ovalbumin in mice," *Vaccine*, vol. 22, pp. 3882-3889, 2004.

[89] P. S. Stayton, T. Shimoboji, C. Long, A. Chilkoti, G. Ghen, J. M. Harris, *et al.*, "Control of protein–ligand recognition using a stimuli-responsive polymer," 1995.

[90] E. M. Bachelder, T. T. Beaudette, K. E. Broaders, S. E. Paramonov, J. Dashe, and J. M. Fréchet, "Acid-degradable polyurethane particles for protein-based vaccines: biological evaluation and in vitro analysis of particle degradation products," *Molecular pharmaceutics*, vol. 5, pp. 876-884, 2008.

[91] S. Han, D. Kim, S.-h. Han, N. H. Kim, S. H. Kim, and Y.-b. Lim, "Structural and Conformational Dynamics of Self-Assembling Bioactive β-Sheet Peptide Nanostructures Decorated with Multivalent RNA-Binding Peptides," *Journal of the American Chemical Society*, vol. 134, pp. 16047-16053, 2012.

[92] D. Mandal, R. K. Tiwari, A. N. Shirazi, D. Oh, G. Ye, A. Banerjee, *et al.*, "Self-assembled surfactant cyclic peptide nanostructures as stabilizing agents," *Soft matter*, vol. 9, pp. 9465-9475, 2013.

[93] V. Manolova, A. Flace, M. Bauer, K. Schwarz, P. Saudan, and M. F. Bachmann, "Nanoparticles target distinct dendritic cell populations according to their size," *European journal of immunology,* vol. 38, pp. 1404-1413, 2008.
[94] J. J. Moon, B. Huang, and D. J. Irvine, "Engineering Nano - and Microparticles to Tune Immunity," *Advanced materials,* vol. 24, pp. 3724-3746, 2012.
[95] U. Boehm, T. Klamp, M. Groot, and J. Howard, "Cellular responses to interferon-γ," *Annual review of immunology,* vol. 15, pp. 749-795, 1997.
[96] A. Yoshida, Y. Koide, M. Uchijima, and T. Yoshida, "IFN-γ induces IL-12 mRNA expression by a murine macrophage cell line, J774," *Biochemical and biophysical research communications,* vol. 198, pp. 857-861, 1994.
[97] C. S. Tannenbaum and T. A. Hamilton, "Immune-inflammatory mechanisms in IFNγ-mediated anti-tumor activity," in *Seminars in cancer biology,* 2000, pp. 113-123.
[98] K. Schroder, P. J. Hertzog, T. Ravasi, and D. A. Hume, "Interferon-γ: an overview of signals, mechanisms and functions," *Journal of leukocyte biology,* vol. 75, pp. 163-189, 2004.
[99] O. Dienz, S. M. Eaton, J. P. Bond, W. Neveu, D. Moquin, R. Noubade, *et al.*, "The induction of antibody production by IL-6 is indirectly mediated by IL-21 produced by CD4+ T cells," *The Journal of experimental medicine,* vol. 206, pp. 69-78, 2009.
[100] P. S. Walker, T. Scharton-Kersten, A. M. Krieg, L. Love-Homan, E. D. Rowton, M. C. Udey, *et al.*, "Immunostimulatory oligodeoxynucleotides promote protective immunity and provide systemic therapy for leishmaniasis via IL-12-and IFN-γ-dependent mechanisms," *Proceedings of the National Academy of Sciences,* vol. 96, pp. 6970-6975, 1999.
[101] R. J. Greenwald, G. J. Freeman, and A. H. Sharpe, "The B7 family revisited," *Annu. Rev. Immunol.,* vol. 23, pp. 515-548, 2005.
[102] D. Verthelyi and R. A. Zeuner, "Differential signaling by CpG DNA in DCs and B cells: not just TLR9," *Trends in immunology,* vol. 24, pp. 519-522, 2003.
[103] A. M. Krieg, "Toll-like receptor 9 (TLR9) agonists in the treatment of cancer," *Oncogene,* vol. 27, pp. 161-167, 2008.
[104] T. Kawabe, M. Matsushima, N. Hashimoto, K. Imaizumi, and Y. Hasegawa, "CD40/CD40 ligand interactions in immune responses and pulmonary immunity," *Nagoya journal of medical science,* vol. 73, pp. 69-78, 2011.
[105] E. Erikçi, M. Gursel, and İ. Gürsel, "Differential immune activation following encapsulation of immunostimulatory CpG oligodeoxynucleotide in nanoliposomes," *Biomaterials,* vol. 32, pp. 1715-1723, 2011.
[106] S. T. Reddy, A. J. van der Vlies, E. Simeoni, V. Angeli, G. J. Randolph, C. P. O'Neil, *et al.*, "Exploiting lymphatic transport and complement activation in nanoparticle vaccines," *Nature biotechnology,* vol. 25, pp. 1159-1164, 2007.
[107] W. R. Heath and F. R. Carbone, "Cross-presentation in viral immunity and self-tolerance," *Nature Reviews Immunology,* vol. 1, pp. 126-134, 2001.
[108] J. J. Engelhardt, B. Boldajipour, P. Beemiller, P. Pandurangi, C. Sorensen, Z. Werb, *et al.*, "Marginating dendritic cells of the tumor microenvironment cross-present tumor antigens and stably engage tumor-specific T cells," *Cancer cell,* vol. 21, pp. 402-417, 2012.

[109] N. van Montfoort, E. van der Aa, and A. M. Woltman, "Understanding MHC class I presentation of viral antigens by human dendritic cells as a basis for rational design of therapeutic vaccines," *Frontiers in immunology,* vol. 5, p. 182, 2014.
[110] J. A. Hubbell, S. N. Thomas, and M. A. Swartz, "Materials engineering for immunomodulation," *Nature,* vol. 462, pp. 449-460, 2009.